Search for the pair production of third-generation squarks with two-body decays to a bottom or charm quark and a neutralino in proton–proton collisions at $\sqrt{s} = 13\,\text{TeV}$

The CMS Collaboration[⋆]

CERN, Switzerland

A B S T R A C T

Results are presented from a search for the pair production of third-generation squarks in proton–proton collision events with two-body decays to bottom or charm quarks and a neutralino, which produces a significant imbalance in the transverse momentum. The search is performed using a sample of proton–proton collision data at $\sqrt{s} = 13\,\text{TeV}$ recorded by the CMS experiment at the LHC, corresponding to an integrated luminosity of $35.9\,\text{fb}^{-1}$. No statistically significant excess of events is observed beyond the expected contribution from standard model processes. Exclusion limits are set in the context of simplified models of bottom or top squark pair production. Models with bottom squark masses up to 1220 GeV are excluded at 95% confidence level for light neutralinos, and models with top squark masses of 510 GeV are excluded assuming that the mass splitting between the top squark and the neutralino is small.

© 2018 The Author. Published by Elsevier B.V. This is an open access article under the CC BY license (http://creativecommons.org/licenses/by/4.0/). Funded by SCOAP³.

1. Introduction

The standard model (SM) has been extremely successful in describing particle physics phenomena. Nevertheless, it suffers from shortcomings such as the hierarchy problem [1], the need for a fine-tuned cancellation of large quantum corrections to the Higgs mass to maintain a physical value at the observed electroweak scale. Supersymmetry (SUSY) [2–9] postulates a symmetry between bosons and fermions and provides a "natural" solution to the hierarchy problem through the cancellation of quadratic divergences in particle and SUSY particle loop corrections to the Higgs boson mass. In natural SUSY models, light top and bottom squarks are preferred with masses close to the electroweak scale [1,10]. In *R*-parity conserving SUSY models [11], SUSY particles are created in pairs, and the lightest SUSY particle (LSP) is stable. The LSP is assumed here to be the lightest neutralino ($\widetilde{\chi}_1^0$), which is both weakly interacting and stable and therefore has the properties of a dark matter candidate [12].

This letter presents searches for the direct production of pairs of bottom ($\widetilde{b}_1\overline{\widetilde{b}}_1$) and top ($\widetilde{t}_1\overline{\widetilde{t}}_1$) squarks, decaying to multijet final states with a large transverse momentum imbalance. The search is performed using $35.9\,\text{fb}^{-1}$ of data collected in proton–proton

(pp) collisions by the CMS detector, at a centre-of-mass energy of 13 TeV, at the CERN LHC [13].

The search for bottom squark pair production is based on the decay mode $\widetilde{b}_1 \to b\widetilde{\chi}_1^0$. This study considers a scenario for top-squark decay that can arise when the mass splitting, $\Delta m \equiv m_{\widetilde{t}_1} - m_{\widetilde{\chi}_1^0}$ is below the mass of the W boson. The decay process $\widetilde{t}_1 \to t\widetilde{\chi}_1^0, t \to bW$ is then suppressed not only because the top quark must be virtual, but also because the W boson must be virtual as well. If flavor-changing neutral current decays $\widetilde{t}_1 \to c\widetilde{\chi}_1^0$ are allowed, then the branching fraction for the two-body decay $\widetilde{t}_1 \to c\widetilde{\chi}_1^0$ can in principle become substantial. Bottom and top squark pair productions are studied in the context of simplified models [14–16]. Fig. 1 illustrates the bottom and top squark decay modes explored in this letter.

The search techniques are based on the work presented in Ref. [17] but use improved discrimination tools to exploit specific kinematic characteristics of the signal models. A charm quark tagging algorithm is used in the top squark search to identify c quarks originating from top squark decays. In addition, specific object reconstruction tools are employed to improve sensitivity to compressed spectrum scenarios, where visible decay products carry low momenta. The new methods and discriminators, as well as the increase in integrated luminosity, lead to considerably improved sensitivity relative to previous searches. While the analysis improvement for compressed spectra is due to the charm and
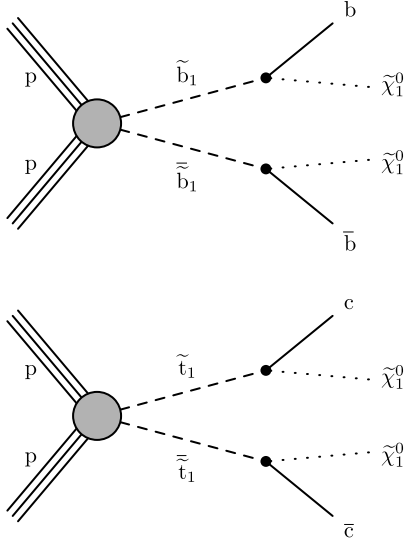
Fig. 1. Diagrams showing the pair production of bottom or top squarks followed by their decays according to $\widetilde{b} \to b\widetilde{\chi}_1^0$ (upper) and $\widetilde{t} \to c\widetilde{\chi}_1^0$ (lower).

soft b quark identification, the increase in the luminosity provides the improved sensitivity for the noncompressed spectra. Results of similar searches were previously reported by the ATLAS and CMS Collaborations, using pp collisions at 7, 8, and 13 TeV [18–38], as well as by the CDF and D0 Collaborations in proton–antiproton collisions at the Fermilab Tevatron [39–42].

2. The CMS detector

The central feature of the CMS detector is a superconducting solenoid of 6 m internal diameter, providing a magnetic field of 3.8 T. An all-silicon pixel and strip tracker, a lead tungstate crystal electromagnetic calorimeter (ECAL), and a brass and scintillator hadron calorimeter, each composed of a barrel and two endcap sections are located within the field volume. Forward calorimeters extend the pseudorapidity (η) coverage provided by the barrel and endcap detectors. Muons are measured in gas-ionization detectors embedded in the steel flux-return yoke outside the solenoid. The first level of the CMS trigger system, composed of specialized hardware processors, uses information from the calorimeters and muon detectors to select the most interesting events in a fixed time interval of less than 4 μs. A high level trigger processor farm decreases the event rate from around 100 kHz to less than 1 kHz, before data storage [43]. A more detailed description of the CMS detector, together with a definition of the coordinate system and relevant kinematic variables, can be found in Ref. [44].

3. Event reconstruction and Monte Carlo simulation

Events are reconstructed with the particle flow (PF) algorithm [45], which combines information from the subdetectors to optimize reconstruction and identification of produced stable particles, namely charged and neutral hadrons, photons, electrons, and muons. Events selected for this search are required to pass filters designed to remove detector- and beam-related noise and must have at least one reconstructed vertex. Usually more than one such vertex is reconstructed, due to pileup, i.e. multiple pp collisions within the same or neighbouring bunch crossings. The reconstructed vertex with the largest value of summed physics-object p_T^2 is taken to be the primary pp interaction vertex (PV), where p_T is the transverse momentum. The physics objects are the objects returned by a jet finding algorithm [46,47] applied to

all charged tracks associated with the vertex, plus the corresponding associated missing transverse momentum.

Charged particles originating from the primary vertex, photons, and neutral hadrons are clustered into jets using the anti-k_T algorithm [46] implemented in FASTJET [47] with a distance parameter of 0.4. The jet energy is corrected for the contribution from pileup based on the jet area method [48]. Additional corrections to the jet energy scale are applied to compensate for variations in detector response [49]. Jets are required to have p_T greater than 25 GeV and to be contained within the tracker volume, $|\eta| < 2.4$. The momentum imbalance vector ($\vec{p}_T^{\text{miss}}$) is calculated as the negative vector sum of transverse momenta of all PF candidates reconstructed in an event, and its magnitude is referred to as missing transverse momentum, denoted p_T^{miss} [50].

Muons are reconstructed by combining the information from the silicon tracker and the muon detectors in a global fit. An identification selection is performed using the quality of the geometrical matching between the tracker and the muon system measurements [51]. Electron candidates are reconstructed by matching clusters of energy deposited in the ECAL to reconstructed tracks. Selection criteria based on the distribution of the shower shape, track cluster matching, and consistency between the cluster energy and track momentum are then used in the identification of electron candidates [52]. Muon and electron candidates are required to have $p_T > 10$ GeV, to be within $|\eta| < 2.4$, and to originate from within 2 mm of the beam axis in the transverse plane. Relative lepton isolation, I_{rel}, is quantified as the sum of the p_T of PF candidates within a cone $\Delta R = \sqrt{(\Delta\eta)^2 + (\Delta\phi)^2}$ around the lepton (where ϕ is the azimuthal angle in radians), divided by the lepton p_T. The lepton itself and charged PF candidates not originating from the PV are not considered in the sum. The isolation sum is corrected for effects of pileup interactions through an area-based estimate [53] of the pileup energy deposited in the cone. The size of the cone is defined according to lepton p_T, as follows:

$$\Delta R = \begin{cases} 0.2, & \text{if } p_T < 50\,\text{GeV}, \\ 10\,\text{GeV}/p_T, & \text{if } 50 < p_T < 200\,\text{GeV}, \\ 0.05, & \text{if } p_T > 200\,\text{GeV}. \end{cases} \quad (1)$$

The shrinking cone radius for higher-p_T leptons maintains high efficiency for the collimated decay products of highly-boosted heavy objects.

Jets are identified as b tagged using the combined secondary vertex (CSVv2) algorithm [54,55]. The b quark jet ("b jet") identification efficiencies for jets with $p_T > 25$ GeV and $|\eta| < 2.4$ vary with jet p_T and are 80–85% and 46–74% for the loose and medium working points used in this analysis, respectively. The probability for light-flavour (charm) jets to be mistagged as function of jet p_T is 8–12% (40%) for the loose working point and 1–2% (20%) for medium working point. The single muon t$\bar{\text{t}}$ events are used to extract the charm mistag rate of the CSVv2 algorithm [55].

A c quark tagging algorithm is used to identify jets originating from charm quarks ("c jets"), while rejecting either b or light-flavour jets [56]. Two classifiers are introduced, one to discriminate c jets from light-flavour, and one for discriminating c jets from b jets. To identify c jets, a selection is implemented in the plane of the two discriminators. As c-jet properties are often distributed in between those of b- and light-jets, the charm tagger discriminators are less efficient than b-tagger and usually suffers from large misidentification rates. We get the best analysis sensitivity using the "medium" working point version of the algorithm, which has 40% c quark identification efficiency for jets with $p_T > 25$ GeV and $|\eta| < 2.4$. The rate for b and light-flavour jets to be mistagged as a c jet is 20%. The efficiency to identify c jets is measured with a

sample enriched in c jets using events with a W boson produced in association with a c quark.

For the very compressed spectra ($m_{\widetilde{b}_1} - m_{\widetilde{\chi}_1^0} < 25\,\text{GeV}$), a large fraction of events contain b quarks with $p_T < 25\,\text{GeV}$, which may fail to pass the jet selection or the b tagging working points. We therefore extend the identification of b quarks based on the presence of a secondary vertex (SV) reconstructed using the inclusive vertex finder (IVF) algorithm [57]. To suppress the background originating from light-flavour jets, the following requirements are placed on the SV observables: the distance in the transverse plane between the SV and PV must be $<3\,\text{cm}$; there must be >2 tracks associated with the SV; the significance of this distance is required to be >4; the cosine of the pointing angle, which is defined through the scalar product between the distance vector $\overrightarrow{(\text{SV}, \text{PV})}$ and the $\vec{p}_{\text{SV}}$ direction has to be >0.98, where $\vec{p}_{\text{SV}}$ is the total three-momentum of the tracks associated with the SV. Finally, in order to avoid overlaps with the b and c tagging selections described above, the distance ΔR of the SV to jets (including b- or c-tagged jets) has to be >0.4, and the transverse component of p_{SV} is required to satisfy $p_{\text{SV}} < 25\,\text{GeV}$. The method has 20% efficiency in identifying b hadrons versus less than one percent of misidentification and the performance in simulation agrees with the performance with data within 16% [58].

The Monte Carlo (MC) simulation of events is used to study the properties of SM backgrounds and signal models. The Mad-Graph5_amc@nlo 2.2.2 generator [59] is used in leading-order (LO) mode to simulate events originating from t$\bar{\text{t}}$, W+jets, Z+jets, and quantum chromodynamics multijet processes ('QCD'), as well as signal events, based on LO NNPDF3.0 [60] parton distribution functions (PDFs). The LO MC is used for these SM processes because it allows a better control of the associated jet production to large multiplicities, while any next-to-leading order (NLO) MC would only model the first radiation at NLO and then use parton shower for extra jets. Single top quark events produced in the tW channel are generated at NLO with Powheg v2 [61–64], while SM processes such as WZ, ZZ, WW, t$\bar{\text{t}}$Z, and t$\bar{\text{t}}$W, which are grouped together as the rare processes because of the small contribution in this analysis, are generated at NLO using the MadGraph5_amc@nlo 2.2.2 program, using NLO NNPDF3.0 PDFs. Parton showering and hadronization is generated using Pythia8.212 [65]. The response of the CMS detector for the SM backgrounds is simulated with the Geant4 [66] package. The CMS fast simulation package [67] is used to simulate all signal samples, and is verified to provide results that are consistent with those obtained from the full Geant4-based simulation. Any residual differences in the detector response description between the Geant4 and fast simulation are corrected for, with corresponding uncertainties in the signal acceptance taken into account. Event reconstruction is performed in the same manner as for collision data. A distribution of pileup interactions is used when producing the simulated samples. The samples are then reweighted to match the pileup profile observed in the collected data. The signal production cross sections are calculated using NLO with next-to-leading logarithm (NLL) soft-gluon resummation calculations [68]. The most precise cross section calculations are used to normalize the SM simulated samples, corresponding most often to next-to-next-to-leading order (NNLO) accuracy.

4. Event selection

The recorded events are required to have $p_T^{\text{miss}} > 100\,\text{GeV}$ at the trigger level. To ensure full trigger efficiency, events selected offline are required to have $p_T^{\text{miss}} > 250\,\text{GeV}$, as well as two, three, or four jets. For bottom squark production, only two jets are expected from squark decays. For the model involving top squarks with a

small mass difference relative to the LSP, most decay products have small p_T and therefore the analysis relies on the presence of one or two additional jets from initial-state radiation (ISR). In both cases, the number of high-p_T jets is expected to be small, and therefore events with a fifth jet with p_T above 75 GeV are rejected. The event is discarded if it has more than five jets.

To reduce the SM background from processes with a leptonically decaying W boson, we reject events containing isolated muons (electrons) with $I_{\text{rel}} < 0.10$ ($I_{\text{rel}} < 0.21$). The contribution from hadronically decaying τ leptons (τ_{h}) is reduced by placing a veto on events containing isolated charged-hadron PF candidates (isolated track) with $p_T > 10\,\text{GeV}$, $|\eta| < 2.5$. Candidates are categorized as being isolated if their isolation sum, i.e. the scalar sum of the p_T of charged PF candidates within a fixed cone of $R = 0.3$ around the candidate is smaller than 10% of the candidate p_T.

The dominant SM background sources are Z+jets events with $Z \to \nu\bar{\nu}$ decay and background from W+jets, t$\bar{\text{t}}$, and single top quark processes with leptonic W boson decays. These processes contribute to the search regions when the lepton is not isolated or identified, or is out of kinematical or detector acceptance. In addition, a hadronically decaying τ lepton can be reconstructed as a jet and hence contributes to the signal region. A smaller background contribution comes from QCD multijet events in which large p_T^{miss} originates from jet mismeasurements. The direction of $\vec{p}_T^{\text{miss}}$ in such events is often aligned with one of the mismeasured jets. To suppress this background, the absolute difference in the azimuthal angle ($\Delta\phi_{\text{min}}$) between $\vec{p}_T^{\text{miss}}$ and the closest of the three jets with highest (i.e. leading) p_T is required to be >0.4.

Two sets of search regions are defined to optimize the sensitivity for signal with either compressed or noncompressed mass spectra. In addition to the criteria discussed above, in models with noncompressed mass spectra we require the p_T of the leading jet to be $>100\,\text{GeV}$ and to contain at least one additional jet with $p_T > 75\,\text{GeV}$. We also require the two leading jets to be b tagged. These requirements suppress events originating from W and Z boson production, in which the leading jets have softer p_T spectra, as they are produced by ISR. To maintain a stable b tagging efficiency as a function of jet p_T, both the loose and medium working points of the b tagging algorithm are used to identify b jets. The b tagging efficiency of the medium working point depends strongly on the jet p_T and degrades by about 20–30% for jets with $p_T > 500\,\text{GeV}$, while the efficiency of the loose working point is more stable with increasing jet p_T. Specifically, we use the loose working point to identify a leading b-tagged jet if it has $p_T > 500\,\text{GeV}$, and otherwise use the medium working point. Since such high-p_T jets are less likely to occur in SM processes, the higher misidentification rate of the loose working point provides only a small increase in the SM background. The third and fourth jet if present, are required to have $p_T > 30\,\text{GeV}$.

In t$\bar{\text{t}}$ events with a lost lepton, the transverse mass distribution of the neutrino and b quark from the same top quark decay has an endpoint at the mass of the top quark. The observable $M_T^{\text{min}}(p_T(\text{j}_{1,2}), p_T^{\text{miss}})$ is defined as

$$M_T^{\text{min}}(p_T(\text{j}_{1,2}), p_T^{\text{miss}}) \equiv \\ \min[M_T(p_T(\text{j}_1), p_T^{\text{miss}}), M_T(p_T(\text{j}_2), p_T^{\text{miss}})], \quad (2)$$

where

$$M_T(p_T(\text{j}_{1,2}), p_T^{\text{miss}}) = \sqrt{2p_T(\text{j}_{1,2})(1 - \cos\Delta\phi(\text{j}_{1,2}, p_T^{\text{miss}}))},$$

$p_T(\text{j}_1)$ and $p_T(\text{j}_2)$ are the transverse momenta of the two leading jets, and $\Delta\phi(\text{j}_{1,2}, p_T^{\text{miss}})$ is the azimuthal angle between leading (sub-leading) jet and $\vec{p}_T^{\text{miss}}$. Imposing a minimum requirement of

Table 1
A summary of the baseline selections used for the noncompressed and compressed search regions.

	Search regions	
	Noncompressed	Compressed
N_{jets}	2–4 ($p_T > 30\,\text{GeV}$)	2–4 ($p_T > 25\,\text{GeV}$)
Jet veto	5th-jet ($p_T > 75\,\text{GeV}$)	5th-jet ($p_T > 75\,\text{GeV}$)
Lepton veto	e, μ, and isolated track	e, μ, and isolated track
Leading jet	$p_T > 100\,\text{GeV}$ and is b tagged	$p_T > 100\,\text{GeV}$ and is not b or c tagged
Sub-leading jet	$p_T > 75\,\text{GeV}$ and is b tagged	$p_T > 25(50)\,\text{GeV}$ and is (is not) b or c tagged
p_T^{miss}	$>250\,\text{GeV}$	$>250\,\text{GeV}$
p_T (ISR)	–	$>250\,\text{GeV}$
$\Delta\phi_{\min}$	$>0.4\,\text{rad}$	$>0.4\,\text{rad}$
$\lvert(\vec{p}_T(\text{ISR}) + \vec{p}_T^{\text{miss}})\rvert/p_T^{\text{miss}}$	–	<0.5
$M_T^{\min}(p_T(\text{j}_{1,2}), p_T^{\text{miss}})$	$>250\,\text{GeV}$	–
M_{CT}	$>150\,\text{GeV}$	–

250 GeV on $M_T^{\min}(p_T(\text{j}_{1,2}), p_T^{\text{miss}})$ reduces a significant portion of the t$\bar{\text{t}}$ background.

Events in this sample are then categorized by H_T, defined as the scalar sum of the p_T of the two leading jets, and the boost-corrected contransverse mass [69,70], M_{CT}, defined as:

$$M_{\text{CT}}^2(\text{j}_1, \text{j}_2) = 2p_T(\text{j}_1)p_T(\text{j}_2)(1 + \cos\Delta\phi(\text{j}_1, \text{j}_2)), \qquad (3)$$

where $\Delta\phi(\text{j}_1, \text{j}_2)$ is the azimuthal angle between two leading jets. For models in which particles are pair produced and have the same decay chain, the M_{CT} distribution has an endpoint determined by the masses of the parent and daughter particles. For the decay $\widetilde{\text{b}}_1 \to \text{b}\widetilde{\chi}_1^0$, this endpoint is at mass $(m_{\widetilde{\text{b}}_1}^2 - m_{\widetilde{\chi}_1^0}^2)/m_{\widetilde{\text{b}}_1}$. A minimum requirement of 150 GeV on M_{CT} is applied.

For signals with compressed mass spectra, high-p_T ISR jet is required to reconstruct the decay chain of quarks as jets and to obtain a large value of p_T^{miss}. Since such ISR jets are not expected to originate from b or c quarks, the leading jet is required to fail the loose b tagging and medium c tagging requirements to define the ISR system according to whether the sub-leading jet is b- or c-tagged. If the next-to-leading jet p_T in the event is $>50\,\text{GeV}$ and is neither b- or c-tagged, the ISR system is defined by the two leading jets; otherwise only the leading jet is considered as the ISR system. The ISR system p_T is required to exceed 250 GeV. The jet imbalance in the transverse plane is quantified as the vector sum of the ISR system $\vec{p}_T$ and $\vec{p}_T^{\text{miss}}$, divided by p_T^{miss}, $\lvert(\vec{p}_T(\text{ISR}) + \vec{p}_T^{\text{miss}})\rvert/p_T^{\text{miss}}$. For the topology of interest, the transverse momentum imbalance must be small and we therefore require that $\lvert(\vec{p}_T(\text{ISR}) + \vec{p}_T^{\text{miss}})\rvert/p_T^{\text{miss}} < 0.5$.

The b- or c-tagged jet, using medium b and c tagging requirements, must have $p_T > 25\,\text{GeV}$, and if a b-tagged jet is also identified as c-tagged jet, it is only counted once as a b-tagged jet.

The M_{CT} observable loses its discriminating power in the compressed models when the mass splitting between the parent particle and the $\widetilde{\chi}_1^0$ is small. Therefore, we use as the main discriminants the number of b- and c-tagged jets ($N_{\text{b-tags}}$ and $N_{\text{c-tags}}$, respectively) and a number of selected SVs (N_{SV}) and p_T^{miss}. If there are at least one b- or c-tagged jets the extra variables, H_T^{b}, and H_T^{c}, which reflect the scalar sums of transverse momenta of b- and c-tagged jets, respectively, are used. The search region with $N_{\text{SV}} > 0$ provides the sensitivity in the very compressed spectra for the bottom squark search.

The baseline selections in both the noncompressed and compressed regions are summarized in Table 1, and the signal region definitions in both regions are shown in Tables 2 and 3, respectively.

The discriminating power of the kinematic quantities used in the analysis is shown in Figs. 2 and 3. In the noncompressed region, the distributions of M_{CT} and $p_T(\text{j}_1) + p_T(\text{j}_2)$, after applying

Table 2
The categorization of H_T and M_{CT} for search regions in noncompressed signal models.

Noncompressed regions	
H_T [GeV]	M_{CT} [GeV]
200–500	150–250, 250–350, 350–450, >450
500–1000	150–250, 250–350, 350–450, 450–600, >600
>1000	150–250, 250–350, 350–450, 450–600, 600–800, >800

all selection requirements (defined in Table 1), are shown in Fig. 2. The combined number of b-, c-tagged jets and SV multiplicity for all events passing selection requirements in the compressed region is shown in the left panel of Fig. 3. The p_T^{miss} distribution for the events with at least one b- or c-tagged jet is shown in the right panel of Fig. 3.

5. Background estimation

The SM background contributions originating from $Z \to \nu\bar{\nu}$, W+jets, t$\bar{\text{t}}$, single-top-quark and QCD multijet processes are estimated from dedicated data control regions as discussed below. Smaller contributions from other, rarer SM processes are estimated from simulation, and a conservative uncertainty of 50% is assigned to these contributions [17]. In this paper the background from W+jets, t$\bar{\text{t}}$, and single top quark processes, is referred to as "lost-lepton background".

5.1. $Z \to \nu\bar{\nu}$ background estimation

The $Z \to \nu\bar{\nu}$ background is estimated from a high-purity data sample of $Z \to \ell^+\ell^-$ events in which we remove the leptons and recalculate the relevant kinematic variables to emulate $Z \to \nu\bar{\nu}$ events. The triggers used to collect this control sample require the presence of one or two muons or two electrons. For the single-muon trigger, the muon must have $p_T > 50\,\text{GeV}$; for the double muon (electron) triggers, the two highest-p_T muons (electrons) must have $p_T > 17\,\text{GeV}$ (23 GeV), and 8 GeV (12 GeV), respectively. The single muon trigger is used to recover a few percent efficiency loss that affects the double muon trigger in the high p_T muon region ($p_T > 400\,\text{GeV}$). In keeping with the trigger constraints, the sample is selected by requiring the presence of two isolated leptons in the event with $|\eta| < 2.4$, and with $p_T > 25$ or $>20\,\text{GeV}$ for the leading and subleading leptons, respectively. The invariant mass of the opposite-charge and same-flavour dilepton pair is required to be within 15 GeV of the Z boson mass [71]. Each lepton is required to be separated from jets in the event by $\Delta R > 0.3$.

Apart from the lepton selection in the $Z \to \ell^+\ell^-$ control sample, the same object and event selection criteria, as described in Section 4, are applied to these events, which are subdivided into

Table 3

The categorization in $N_{\text{b-tags}}$, $N_{\text{c-tags}}$, N_{SV}, H_{T}, and $p_{\text{T}}^{\text{miss}}$ for search regions in models with compressed spectra. Only events with zero b-tagged jets are used to define the search regions with exactly one or two c-tagged jets.

Compressed regions		
$N_{\text{b-tags}}$, $N_{\text{c-tags}}$, N_{SV}	$p_{\text{T}}^{\text{miss}}$ [GeV]	H_{T} (b- or c-tagged jets) [GeV]
$N_{\text{b-tags}} = 1$	250–300	<100
	300–500	<100
	500–750	<100
	750–1000	<100
	>1000	<100
$N_{\text{b-tags}} = 2$	250–300	<100
		100–200
	300–500	<100
		100–200
	>500	<100
		100–200
$N_{\text{c-tags}} = 1$	250–300	<100
	300–500	<100
	500–750	<100
	750–1000	<100
	>1000	<100
$N_{\text{c-tags}} = 2$	250–300	<100
		100–200
	300–500	<100
		100–200
	500–750	<100
		100–200
	>750	<100
		100–200
$N_{\text{b-tags}} + N_{\text{c-tags}} + N_{\text{SV}} = 0$	300–500	–
	500–750	–
	750–1000	–
	1000–1250	–
	>1250	–
$N_{\text{b-tags}} + N_{\text{c-tags}} = 0$, $N_{\text{SV}} > 0$	250–300	–
	300–500	–
	500–750	–
	750–1000	–
	>1000	–

control regions, corresponding to the noncompressed and compressed search regions.

The expected number of $Z \to \nu\bar{\nu}$ events in each signal region is then obtained by scaling the simulated yield, $N_{Z \to \nu\bar{\nu}}^{\text{MC}}$, by scale and shape correction factors, according to:

$$N_{Z \to \nu\bar{\nu}}^{\text{Pred}} = N_{Z \to \nu\bar{\nu}}^{\text{MC}} \frac{N_{Z \to \ell^+\ell^-}^{\text{data}}}{N_{Z \to \ell^+\ell^-}^{\text{MC}}} S_{\text{data/MC}}. \tag{4}$$

The term $N_{Z \to \ell^+\ell^-}^{\text{data}} / N_{Z \to \ell^+\ell^-}^{\text{MC}}$ is a scale factor to account for data-MC differences in the dilepton selection. It is computed for each $N_{\text{b-tags}}$, $N_{\text{c-tags}}$, and N_{SV} category separately, with an inclusive selection in the kinematic variables M_{CT}, $p_{\text{T}}^{\text{miss}}$, and H_{T} to improve statistical precision. The term $S_{\text{data/MC}}$ is a shape correction factor that accounts for possible differences in the shape of the kinematic variables used to define the signal regions. To compensate for the low event count due to the low branching fraction of the Z boson to dilepton final states, relaxed heavy flavor tagging requirements are used to compute the shape corrections. In the noncompressed region, jets are b tagged using a loose working point, while in the compressed region an inclusive $N_{\text{b-tags}}$, $N_{\text{c-tags}}$, and N_{SV} selec-

tion is used. The shape correction factors in the noncompressed region are determined via comparison of the M_{CT} distribution in $Z \to \ell^+\ell^-$ events in simulation and data. To do the comparison, we first normalize the simulation to the number of observed events in data after applying the loose selection criteria. The small contamination from $t\bar{t}$, W+jets, single top quark and rare processes is estimated using simulation and subtracted from data. The size of shape corrections in the noncompressed region varies between 3 to 20% from lowest to highest M_{CT} bin. After applying the shape correction factor in bins of M_{CT} and similar selections as in the search regions, good agreement between the data and simulation is found as a function of $p_{\text{T}}^{\text{miss}}$ and H_{T}. In the given H_{T} bin, the small residual difference in the H_{T} distribution is considered as a systematic uncertainty. In addition to the shape correction factors, the scale factor is calculated in the $Z \to \ell^+\ell^-$ control sample using the same b tagging requirements as in the signal region, and the value is determined to be consistent with unity within the statistical uncertainty.

For compressed regions, the shape correction factors are calculated inclusively in $N_{\text{b-tags}}$, $N_{\text{c-tags}}$, and N_{SV} as a function of $p_{\text{T}}^{\text{miss}}$ in the same way as in the noncompressed regions. The typical range
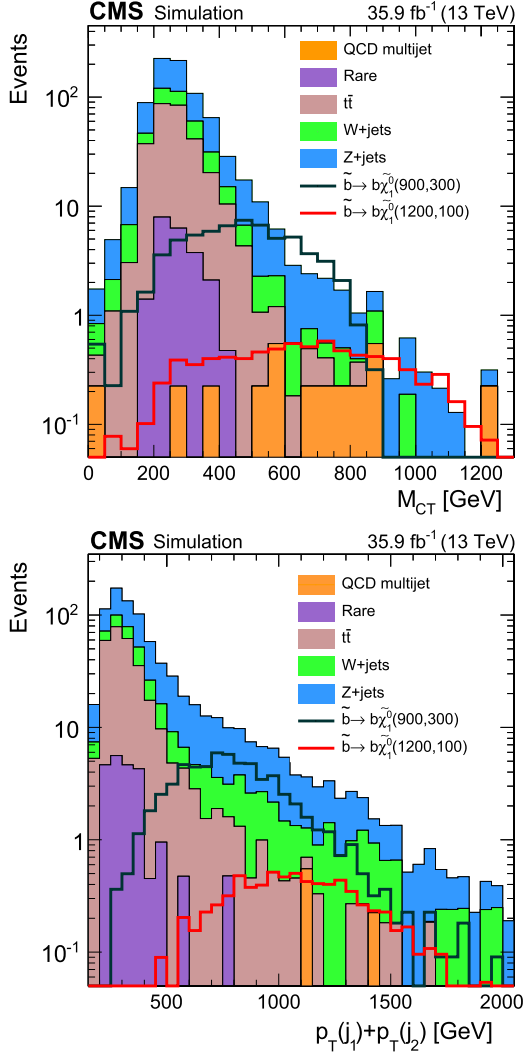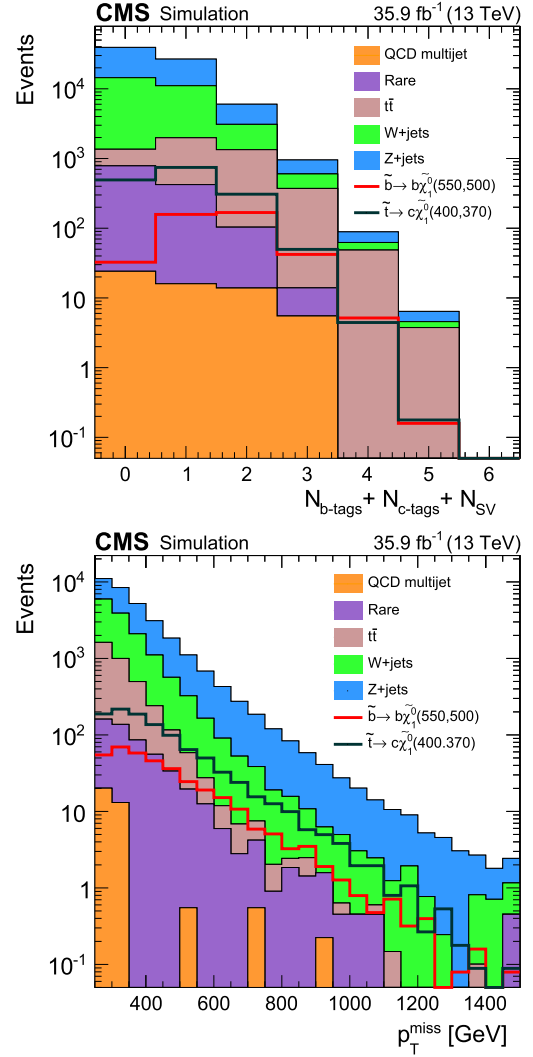
Fig. 2. Distribution of M_{CT} (upper) and $p_T(j_1) + p_T(j_2)$ (lower) for the searches in noncompressed regions from simulation. The stacked, filled histograms represent different background components while the lines show two signal models with different bottom squark and neutralino mass hypotheses ($m_{\tilde{b}} = 900\,\text{GeV}$ and $m_{\tilde{\chi}_1^0} = 300\,\text{GeV}$) and ($m_{\tilde{b}} = 1200\,\text{GeV}$ and $m_{\tilde{\chi}_1^0} = 100\,\text{GeV}$). (For interpretation of the references to colour in this figure, the reader is referred to the web version of this article.)

of shape corrections in the compressed region is 5 to 70%. The scale factors are determined in each $N_{b\text{-tags}}$, $N_{c\text{-tags}}$, and N_{SV} signal region separately, and are consistent with unity within the statistical uncertainties.

Two sources of systematic uncertainty in the $Z \to \nu\bar{\nu}$ background contribution are uncertainties related to the use of simulation and uncertainties in the methods used to predict the background. The first set of uncertainties is related to the choice of the renormalization and factorization scales, PDFs, jet and p_T^{miss} energy scale, and the uncertainties in scale factors to correct the differences between the data and simulation in b or c tagging, and lepton identification and isolation efficiencies. The total uncertainty from these sources is in the range of 1–20%, depending on the signal region.

The second set of systematic uncertainties has a larger impact on the prediction, varies from 10 to 100%, is due to the statistical uncertainties in the normalization and scale factors, contamination of other background sources in dilepton sample, the effect of the difference in the H_T shape, and the uncertainty related to the trigger efficiency.

Fig. 3. Distributions of the combined b-, c-tagged jet, and SV multiplicity (upper), and p_T^{miss} for events with at least one b- or c-tagged jet (lower), after the baseline selection for the compressed mass spectrum analysis, as obtained from simulation. The stacked, filled histograms represent different background components while the lines show two signal models with different bottom and top squark and neutralino mass hypotheses ($m_{\tilde{b}} = 550\,\text{GeV}$ and $m_{\tilde{\chi}_1^0} = 500\,\text{GeV}$) and ($m_{\tilde{t}} = 400\,\text{GeV}$ and $m_{\tilde{\chi}_1^0} = 370\,\text{GeV}$). (For interpretation of the references to colour in this figure, the reader is referred to the web version of this article.)

5.2. Lost-lepton background estimation

The lost-lepton background in each search region is estimated from a single-lepton control region in data selected by inverting the muon or electron vetoes in the events collected with the same trigger as used to record the signal sample. The control regions are defined through the same selection criteria as the corresponding search regions, including requirements on H_T, M_{CT}, $N_{b\text{-tags}}$, $N_{c\text{-tags}}$, N_{SV}, and p_T^{miss}, to remove any dependence of the prediction on the modelling of these kinematic variables in simulation. The possible contamination from signal in the single-lepton control region is found to have a negligible effect ($<1\%$). The lost-lepton component of the SM background in each search region, N_{LL}^{pred}, is estimated from the corresponding data via a transfer factor, T_{LL}, determined from simulation:

$$N_{LL}^{Pred} = N_{1\ell}^{data} T_{LL}, \quad T_{LL} = \frac{N_{0\ell}^{MC}}{N_{1\ell}^{MC}}, \tag{5}$$

Table 4
Different systematic uncertainties in the lost-lepton background estimate.

Source	Noncompressed regions (%)	Compressed regions (%)
b tagging efficiency	12–25	8–22
c tagging efficiency	–	11–23
Lepton efficiency	3–4	3–4
τ_h veto	7	7
Transfer factor (statistical uncertainty)	5–60	1–40
Transfer factor (systematic uncertainty)	1–20	15–25
Other SM process contamination	3–5	3–10

where $N_{1\ell}^{\mathrm{data}}$ is the observed event yield in the single-lepton control region and $N_{0\ell}^{\mathrm{MC}}$ and $N_{1\ell}^{\mathrm{MC}}$ are the simulated lost-lepton background yields in the corresponding zero- and single-lepton regions, respectively. The transfer factor T_{LL} accounts for effects related to lepton acceptance and efficiency.

The largest uncertainty in the lost-lepton background estimate is from statistical uncertainties in the event yields, ranging from 1 to 60%, depending on the search region. Contributions to the control regions from $Z \to \ell^+\ell^-$ and rare processes are subtracted using estimates from simulation, where a 50% uncertainty applied to the subtraction that leads to an uncertainty of 3–10% in the lost-lepton background prediction. The uncertainties related to discrepancies between the lepton selection efficiency in data and simulation give rise to a 3–4% uncertainty in the final estimate. An additional uncertainty of 7% in the τ_h component accounts for differences in isolation efficiency between muons and single-prong τ_h decays, as determined from studies with simulated samples of W+jets and $t\bar{t}$ events. A systematic uncertainty of 8–25% is found for the uncertainties in b or c tagging scale factors that are applied to the simulation for the differences in b or c tagging performance between data and simulation.

Finally, we estimate a systematic uncertainty in the transfer factor to account for differences in the $t\bar{t}$ and W+jets composition of the search and control regions. This results in a 1–25% uncertainty in the final prediction.

Table 4 provides a detailed breakdown of the various components of the systematic uncertainties in the noncompressed and compressed regions.

5.3. Multijet background estimation

The $\Delta\phi_{\min} > 0.4$ requirement reduces the QCD multijet contribution to a small fraction of the total background in all search regions for both compressed and noncompressed models. We estimate this contribution for each search region by applying a transfer factor to the number of events observed in control regions enriched in QCD events. The control regions are obtained by inverting the $\Delta\phi_{\min}$ requirement. The transfer factor (T_{QCD}) is the ratio between the number of QCD multijet events in $\Delta\phi_{\min} > 0.4$ to the number of events with $\Delta\phi_{\min} < 0.4$, which is measured in simulation and validated with data in a sideband region with $p_{\mathrm{T}}^{\mathrm{miss}} \in [200, 250]\,\mathrm{GeV}$ and similar selections as in the search regions. The estimated contribution from other SM processes ($t\bar{t}$, W+jets, single top quark, and rare process production) based on simulated samples is subtracted from the event yields in the control region.

The transfer factor for the noncompressed regions does not vary significantly as a function of H_{T} or M_{CT}. Therefore, we extract the value of T_{QCD} used for the noncompressed search regions from simulation and a low-$p_{\mathrm{T}}^{\mathrm{miss}}$ sideband region selected with an inclusive requirement on H_{T} and M_{CT} to reduce the statistical uncertainty in the transfer factor. The transfer factors for the compressed search regions are obtained from simulation and low-$p_{\mathrm{T}}^{\mathrm{miss}}$ side-

bands that are subdivided by the number of b- and c-tagged jets, and selected SV according to $N_{\text{b-tags}} + N_{\text{c-tags}} + N_{\mathrm{SV}} = 0$, $N_{\text{b-tags}} \geq 1$, $N_{\text{c-tags}} \geq 1$, and $N_{\mathrm{SV}} \geq 0$ regions. The $N_{\text{b-tags}} \geq 1$ ($N_{\text{c-tags}} \geq 1$) regions are defined for extracting the QCD multijet background predictions for the $N_{\text{b-tags}}(N_{\text{c-tags}}) = 1$ and $N_{\text{b-tags}}(N_{\text{c-tags}}) = 2$ search regions.

The statistical uncertainties due to the limited number of events in the data control regions and the simulated samples are propagated to the final QCD multijet estimate, and range between 10 to 100%. The main uncertainty in T_{QCD} also originates from the statistical uncertainty of the observed and simulated event yields in the low-$p_{\mathrm{T}}^{\mathrm{miss}}$ sideband region. We assign additional uncertainties for the differences in the b and c tagging efficiencies between data and simulation.

6. Results and interpretation

The expected SM background yields and the number of events observed in data are summarized in Table 5 for the noncompressed search regions, and in Tables 6, 7, and 8 for the compressed search regions. The results are shown in Fig. 4 for both search regions.

The data are consistent with the background expected from the SM processes. The results are interpreted as upper cross section limits on bottom and top squark pair production.

The dominant systematic uncertainties on the signal yield predictions are: the luminosity determination (2.5%) [72], the signal acceptance and efficiency arising from the jet energy corrections (5%); renormalization and factorization scale (5%); ISR modelling (5–20%); trigger efficiency (2%); b and c tagging efficiency (5–30%); and selected SV efficiency (16–50%). The uncertainty of 16% is considered if the selected SV is matched to b hadrons, and it is doubled if the selected SV is matched to c hadrons. Finally, a 50% uncertainty in the selected SV efficiency is applied, if it is not matched to either b or c hadrons. However, due to the small misidentification rate (~1%) the considered 50% uncertainty has a negligible effect on final limits. The statistical uncertainty due to the limited size of the simulated samples, calculated for each signal model, varies from a few percent to 100% and is not correlated with signal systematic uncertainties. While the uncertainties in the b- and c-tagged jet and lepton efficiency corrections in simulation are correlated between different processes and search bins, the uncertainties in transfer factors are treated as fully uncorrelated. For the signal, all systematic uncertainties are correlated between the different search regions. We improve the modelling of ISR jets, which affects the total transverse momentum (p_{T} (ISR)) of the system of SUSY particles, by reweighting the p_{T} (ISR) distribution of signal events. This reweighting procedure is based on studies of the transverse momentum of Z events [26]. The reweighting factors range between 1.18 at p_{T} (ISR) 125 GeV and 0.78 for $p_{\mathrm{T}}(ISR) > 600\,\mathrm{GeV}$. We take the deviation from 1.0 as the systematic uncertainty in the reweighting procedure.

The 49 signal bins in $p_{\mathrm{T}}^{\mathrm{miss}}$, H_{T}, M_{CT}, $N_{\text{b-tags}}$, $N_{\text{c-tags}}$, and N_{SV} are statistically independent, and the correlations among all the

Table 5
Observed number of events and background prediction in the noncompressed regions. The total uncertainties in the background predictions are shown.

Noncompressed regions								
H_T [GeV]	M_{CT} [GeV]	Bin	$Z \to \nu\bar{\nu}$	Lost-lepton	QCD	Rare	Total SM	Data
200–500	150–250	1	123 ± 27	145 ± 27	<0.7	8.8 ± 4.4	278 ± 40	275
	250–350	2	130 ± 26	125 ± 29	$0.96^{+1.67}_{-0.96}$	9.8 ± 4.9	266 ± 40	292
	350–450	3	28.5 ± 9.1	31.6 ± 7.2	$1.06^{+1.57}_{-1.06}$	1.87 ± 0.93	63 ± 12	57
	>450	4	0.64 ± 0.57	0.56 ± 0.46	<0.30	<0.2	1.21 ± 0.79	2
500–1000	150–250	5	21.2 ± 6.6	9.2 ± 3.7	$0.85^{+1.08}_{-0.85}$	0.47 ± 0.24	31.8 ± 7.6	32
	250–350	6	24.2 ± 6.1	12.8 ± 4.5	$0.99^{+1.3}_{-0.99}$	<0.2	37.9 ± 7.8	27
	350–450	7	14.3 ± 3.5	6.1 ± 2.1	$1.2^{+1.6}_{-1.2}$	0.47 ± 0.24	22.2 ± 4.4	30
	450–600	8	19.1 ± 6.2	8.6 ± 2.3	$1.1^{+1.5}_{-1.1}$	<0.2	28.9 ± 6.8	29
	>600	9	4.4 ± 2.4	1.25 ± 0.67	<0.46	<0.2	5.7 ± 2.5	6
>1000	150–250	10	6.6 ± 1.7	5.2 ± 4.1	<0.23	<0.2	11.8 ± 4.4	10
	250–350	11	5.4 ± 1.5	2.8 ± 1.7	$0.37^{+0.53}_{-0.35}$	<0.2	8.6 ± 2.3	9
	350–450	12	2.71 ± 0.82	3.2 ± 1.9	$0.62^{+0.80}_{-0.62}$	<0.2	6.6 ± 2.3	4
	450–600	13	2.3 ± 0.83	0.73 ± 0.65	$0.64^{+0.82}_{-0.64}$	<0.2	3.7 ± 1.3	3
	600–800	14	1.08 ± 0.57	0.12 ± 0.15	<0.13	<0.2	1.22 ± 0.61	0
	>800	15	2.1 ± 1.4	0.38 ± 0.40	<0.21	<0.2	2.5 ± 1.5	0

Table 6
Observed number of events and the background prediction in the compressed regions with $N_{\text{b-tags}} = 1, 2$. The total uncertainties in the background predictions are also shown.

Compressed regions								
p_T^{miss} [GeV]	H_T^b [GeV]	Bin	$Z \to \nu\bar{\nu}$	Lost-lepton	QCD	Rare	Total SM	Data
$N_{\text{b-tags}} = 1$								
250–300	<100	1	555 ± 92	1118 ± 210	26^{+27}_{-26}	21 ± 10	1720 ± 230	1768
300–500	<100	2	1100 ± 130	1195 ± 220	14^{+15}_{-14}	38 ± 19	2348 ± 260	2402
500–750	<100	3	162 ± 21	55 ± 12	<0.33	6.7 ± 3.5	224 ± 25	211
750–1000	<100	4	17.7 ± 4.3	5.7 ± 2.4	<0.15	<0.2	23.4 ± 4.9	19
>750	<100	5	3.6 ± 1.6	0.51 ± 0.50	<0.1	<0.2	4.1 ± 1.7	5
$N_{\text{b-tags}} = 2$								
250–300	<100	6	6.9 ± 2.8	51 ± 12	$0.36^{+0.46}_{-0.36}$	0.47 ± 0.23	59 ± 12	70
250–300	100–200	7	12.9 ± 4.5	120 ± 25	$0.62^{+0.78}_{-0.62}$	<0.2	134 ± 25	127
300–500	<100	8	19.4 ± 6.3	72 ± 17	<0.2	1.36 ± 0.68	92 ± 18	77
300–500	100–200	9	34 ± 10	151 ± 31	<0.2	1.35 ± 0.67	188 ± 32	161
>500	<100	10	2.64 ± 0.98	1.22 ± 0.87	<0.1	<0.2	3.9 ± 1.3	7
>500	100–200	11	8.7 ± 2.9	5.1 ± 2.3	<0.1	0.45 ± 0.22	14.35 ± 3.7	8

Table 7
Observed number of events and the background prediction in the compressed regions with $N_{\text{c-tags}} = 1, 2$. The total uncertainties in the background predictions are also shown.

| Compressed regions								
p_T^{miss} [GeV]	H_T^c [GeV]	Bin	$Z \to \nu\bar{\nu}$	Lost-lepton	QCD	Rare	Total SM	Data
$N_{\text{c-tags}} = 1$								
250–300	<100	1	3022 ± 480	3049 ± 530	20^{+22}_{-20}	85 ± 42	6177 ± 720	6867
300–500	<100	2	5852 ± 690	3622 ± 620	11^{+12}_{-11}	178 ± 89	9664 ± 930	10515
500–750	<100	3	765 ± 95	214 ± 39	<0.2	22 ± 11	1002 ± 100	926
750–1000	<100	4	67 ± 13	16.2 ± 3.9	<0.1	3.7 ± 1.8	88 ± 14	73
>1000	<100	5	16.0 ± 6.9	1.37 ± 0.78	<0.1	0.45 ± 0.22	17.8 ± 7.1	18
$N_{\text{c-tags}} = 2$								
250–300	<100	6	145 ± 33	198 ± 42	$0.98^{+1.1}_{-0.98}$	4.1 ± 2.1	348 ± 54	364
250–300	100–200	7	199 ± 25	238 ± 46	4.3 ± 4.7	7.8 ± 3.9	449 ± 53	508
300–500	<100	8	293 ± 39	229 ± 45	0.81 ± 0.91	9.7 ± 4.8	532 ± 60	547
300–500	100–200	9	489 ± 55	323 ± 59	1.5 ± 1.7	19.3 ± 9.6	833 ± 81	874
500–750	<100	10	44 ± 13	23.4 ± 7.2	<0.1	2.3 ± 1.1	70 ± 15	56
500–750	100–200	11	95 ± 14	31.8 ± 7.8	<0.1	3.7 ± 1.8	130 ± 16	102
>750	<100	12	3.6 ± 1.9	0.52 ± 0.58	<0.1	<0.2	4.1 ± 1.9	2
>750	100–200	13	6.7 ± 2.6	2.9 ± 1.6	<0.1	0.45 ± 0.22	10.1 ± 3.1	8

Table 8

Observed number of events and the background prediction in the compressed regions with $N_{\text{b-tags}} + N_{\text{c-tags}} = 0$. The total uncertainties in the background predictions are also shown.

Compressed regions							
p_T^{miss} [GeV]	Bin	$Z \to \nu\bar{\nu}$	Lost-lepton	QCD	Rare	Total SM	Data
$N_{\text{b-tags}} + N_{\text{c-tags}} + N_{\text{SV}} = 0$							
300–500	1	10676 ± 740	5398 ± 930	148^{+160}_{-150}	320 ± 160	16542 ± 1200	17042
500–750	2	1902 ± 180	414 ± 73	$1.4^{+2.1}_{-1.4}$	39 ± 19	2358 ± 200	2028
750–1000	3	143 ± 21	31.2 ± 6.6	<0.45	6.1 ± 3.1	181 ± 22	171
1000–1250	4	42 ± 16	5.9 ± 2.8	<0.03	0.47 ± 0.23	49 ± 16	33
>1250	5	5.1 ± 5.7	2.3 ± 1.6	$0.09^{+0.17}_{-0.09}$	0.92 ± 0.46	8.4 ± 6.0	9
$N_{\text{b-tags}} + N_{\text{c-tags}} = 0,\ N_{\text{SV}} > 0$							
250–300	6	169 ± 22	179 ± 36	$4.5^{+5.1}_{-4.5}$	3.7 ± 1.9	357 ± 43	331
300–500	7	303 ± 37	210 ± 41	$2.9^{+3.3}_{-2.9}$	6.9 ± 3.4	523 ± 57	509
500–750	8	46.6 ± 6.2	15.1 ± 4.8	$0.03^{+0.13}_{-0.03}$	1.40 ± 0.70	64.2 ± 7.8	52
750–1000	9	5.7 ± 1.2	0.73 ± 0.59	<0.1	<0.2	6.5 ± 1.3	3
>1000	10	1.5 ± 1.1	0.07 ± 0.10	<0.2	0.45 ± 0.22	2.0 ± 1.1	0
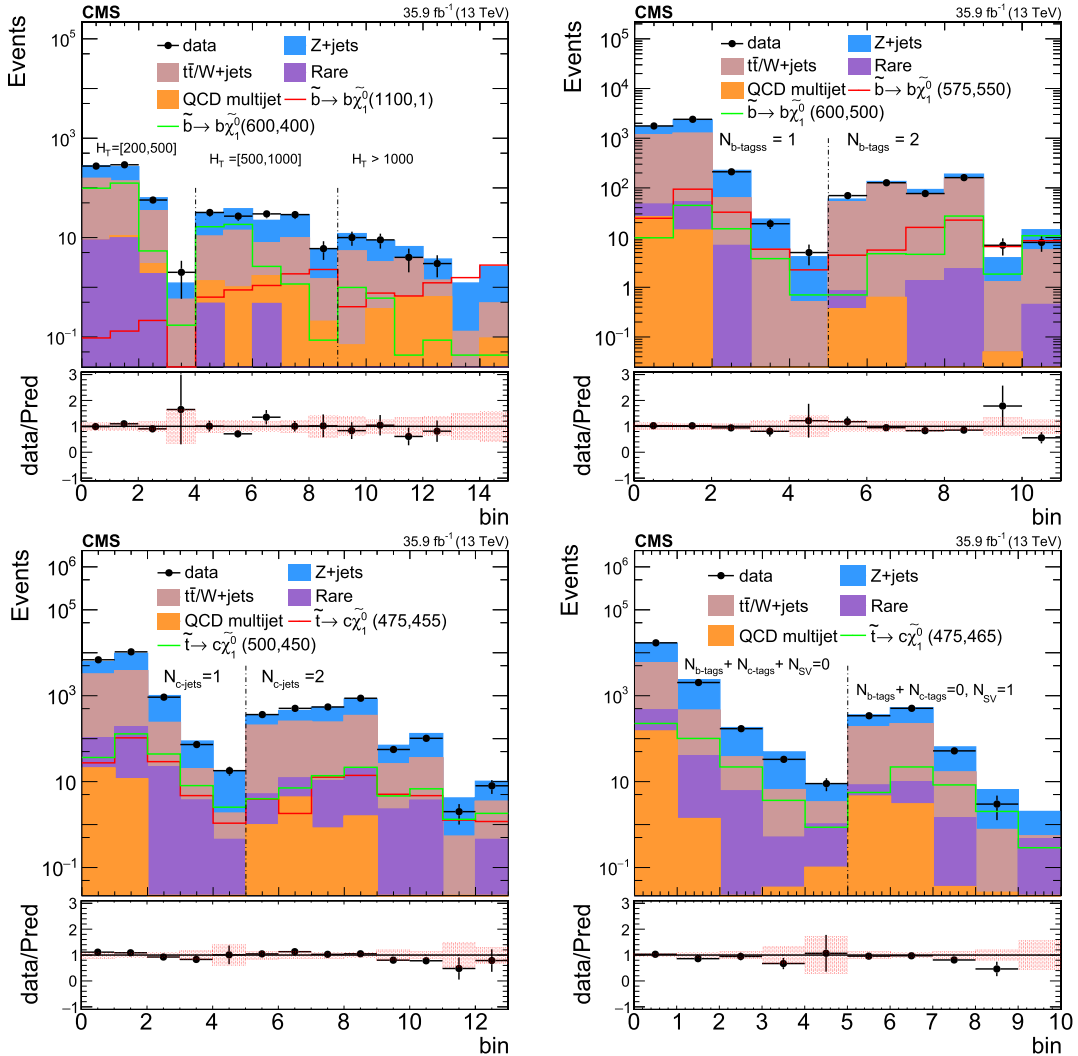
Fig. 4. Yields in the signal regions targeting the noncompressed (top left) and compressed (top right: $N_{\text{b-tags}} = 1, 2$, bottom left: $N_{\text{c-tags}} = 1, 2$, bottom right: $N_{\text{b-tags}} + N_{\text{c-tags}} = 0$) scenarios. Data are shown as black points. The background predictions are represented by the stacked, filled histograms. The expected yields for several signal models are also shown. The lower panels show the ratio of data over total background prediction in each signal region. The hatching indicates the total uncertainty in the background predictions. (For interpretation of the references to colour in this figure, the reader is referred to the web version of this article.)
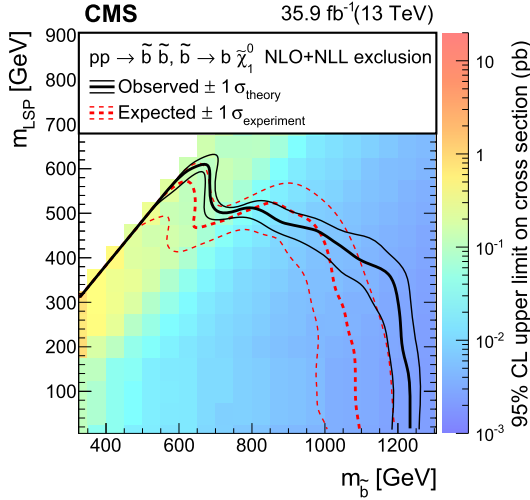
Fig. 5. Exclusion limits at 95% CL for direct bottom squark pair production for the decay mode $\tilde{b}_1 \rightarrow b\tilde{\chi}_1^0$. The regions enclosed by the black curves represent the observed exclusion and the ± 1 standard deviation for the NLO + NLL cross section calculations and their uncertainties [68]. The dashed red lines indicate the expected limits at 95% CL and their ± 1 standard deviation experimental uncertainties. (For interpretation of the references to colour in this figure, the reader is referred to the web version of this article.)

systematic uncertainties in different bins are taken into account. The 95% confidence level (CL) upper limits on SUSY production cross-sections are calculated using a modified frequentist approach with the CL_S criterion [73–75] in which a profile likelihood rate test-statistic is used. The limits are determined using asymptotic approximations for the distributions of the test-statistic [76].

Fig. 5 shows the expected and observed 95% CL upper limits on the bottom squark cross sections, assuming the bottom squark exclusively decays to a bottom quark and an LSP.

Both compressed and noncompressed regions are used to search for the bottom squark, and the compressed search regions are only used to set upper limits on the top squark cross sections when the mass splitting between the top squark and the LSP is smaller than the mass of the W boson. Fig. 6 shows the expected and observed 95% CL upper limits on the top squark cross sections in the $m_{\tilde{t}_1} - m_{\tilde{\chi}_1^0}$ plane assuming the top squark decays exclusively to a charm quark and an LSP. Top squarks with masses below 510 GeV are excluded in this model for a mass splitting between the top squark and the LSP is small. For the similar interpretation [58], top squark and LSP masses are excluded up to 560 and 520 GeV, respectively.

To facilitate reinterpretation, the covariance matrices for the background estimates in the compressed and noncompressed search regions are provided in supplemental Appendix A.

7. Summary

A search for the pair production of third-generation squarks is performed using data collected by the CMS experiment, focusing on two-body decays to bottom or charm quarks. For bottom-squark pair production, the decay mode considered is $\tilde{b}_1 \rightarrow b\tilde{\chi}_1^0$, while for top-squark pair production, the decay mode considered is $\tilde{t}_1 \rightarrow c\tilde{\chi}_1^0$, a flavor-changing neutral current process. No statistically significant excess of events is observed above the expected standard model background, and exclusion limits are set at 95% confidence level in the context of simplified models of direct top and bottom squark pair production. Bottom squark masses below 1220 GeV are excluded assuming that the lightest supersymmetric particle (LSP) is massless; bottom squark masses below 675 GeV
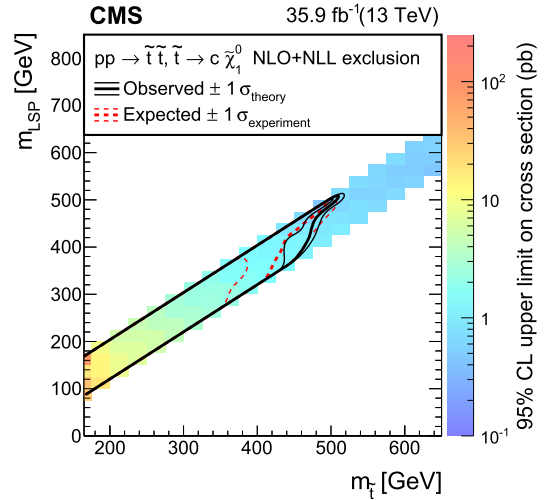
Fig. 6. The combined 95% CL exclusion limits for top squark pair production assuming 100% branching fraction to the decay $\tilde{t} \rightarrow c\tilde{\chi}_1^0$. Notations are as in Fig. 5. (For interpretation of the references to colour in this figure, the reader is referred to the web version of this article.)

are excluded for LSP masses up to 600 GeV. Top squark masses below 510 GeV are excluded for the scenario in which $\tilde{t}_1 \rightarrow c\tilde{\chi}_1^0$ and the mass splitting between the top squark and the LSP is small.

Fig. A.1. The correlation matrix for the estimated backgrounds in the noncompressed search region. The bin numbers are defined in Table 5. (For interpretation of the references to colour in this figure, the reader is referred to the web version of this article.)
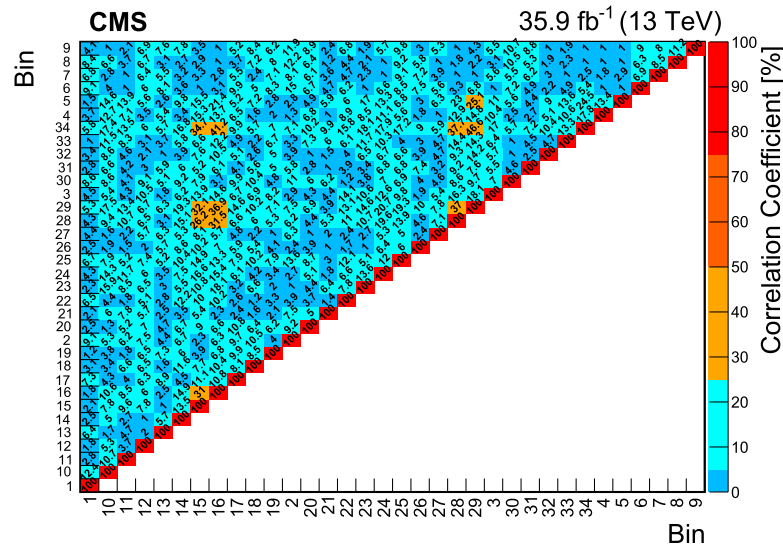
Fig. A.2. The correlation matrix for the estimated backgrounds in the compressed search region. The bin numbers are defined in Table A.1. (For interpretation of the references to colour in this figure, the reader is referred to the web version of this article.)

Table A.1

The bin number and definition for the compressed search region as shown in Fig. A.1 above.

Compressed region			
$N_{\text{b-tags}}, N_{\text{c-tags}}, N_{\text{SV}}$	p_T^{miss} [GeV]	H_T (b- or c-tagged jets) [GeV]	Bin
$N_{\text{b-tags}} = 1$	250–300	<100	1
	300–500	<100	2
	500–750	<100	3
	750–1000	<100	4
	>1000	<100	5
$N_{\text{b-tags}} = 2$	250–300	<100	6
		100–200	7
	300–500	<100	8
		100–200	9
	>500	<100	10
		100–200	11
$N_{\text{c-tags}} = 1$	250–300	<100	12
	300–500	<100	13
	500–750	<100	14
	750–1000	<100	15
	>1000	<100	16
$N_{\text{c-tags}} = 2$	250–300	<100	17
		100–200	18
	300–500	<100	19
		100–200	20
	500–750	<100	21
		100–200	22
	>750	<100	23
		100–200	24
$N_{\text{b-tags}} + N_{\text{c-tags}} = 0, N_{\text{SV}} > 0$	250–300	–	25
	300–500	–	26
	500–750	–	27
	750–1000	–	28
	>1000	–	29
$N_{\text{b-tags}} + N_{\text{c-tags}} + N_{\text{SV}} = 0$	300–500	–	30
	500–750	–	31
	750–1000	–	32
	1000–1250	–	33
	>1250	–	34

Appendix A. Correlation matrices for background estimates

To facilitate reinterpretation of the results in a broader range of beyond the standard model scenarios [77], the correlation matrices for the background estimates in the noncompressed and compressed search regions are provided in Figs. A.1 and A.2, respectively. The bin number in the compressed region is the same as in Table 5 of our paper and in the noncompressed region shown below in Table A.1.

References

[1] R. Barbieri, G.F. Giudice, Upper bounds on supersymmetric particle masses, Nucl. Phys. B 306 (1988) 63, https://doi.org/10.1016/0550-3213(88)90171-X.

[2] P. Ramond, Dual theory for free fermions, Phys. Rev. D 3 (1971) 2415, https://doi.org/10.1103/PhysRevD.3.2415.

[3] Yu.A. Gol'fand, E.P. Likhtman, Extension of the algebra of Poincaré group generators and violation of P invariance, JETP Lett. 13 (1971) 323, http://www.jetpletters.ac.ru/ps/1584/article_24309.pdf.

[4] A. Neveu, J.H. Schwarz, Factorizable dual model of pions, Nucl. Phys. B 31 (1971) 86, https://doi.org/10.1016/0550-3213(71)90448-2.

[5] D.V. Volkov, V.P. Akulov, Possible universal neutrino interaction, JETP Lett. 16 (1972) 438, http://www.jetpletters.ac.ru/ps/1766/article_26864.pdf, Pis'ma Zh. Eksp. Teor. Fiz. 16 (1972) 621.

[6] J. Wess, B. Zumino, A Lagrangian model invariant under supergauge transformations, Phys. Lett. B 49 (1974) 52, https://doi.org/10.1016/0370-2693(74)90578-4.

[7] J. Wess, B. Zumino, Supergauge transformations in four dimensions, Nucl. Phys. B 70 (1974) 39, https://doi.org/10.1016/0550-3213(74)90355-1.

[8] P. Fayet, Supergauge invariant extension of the Higgs mechanism and a model for the electron and its neutrino, Nucl. Phys. B 90 (1975) 104, https://doi.org/10.1016/0550-3213(75)90636-7.

[9] H.P. Nilles, Supersymmetry, supergravity and particle physics, Phys. Rep. 110 (1984) 1, https://doi.org/10.1016/0370-1573(84)90008-5.

[10] M. Papucci, J.T. Ruderman, A. Weiler, Natural SUSY endures, J. High Energy Phys. 09 (2012) 035, https://doi.org/10.1007/JHEP09(2012)035, arXiv:1110.6926.

[11] G.R. Farrar, P. Fayet, Phenomenology of the production, decay, and detection of new hadronic states associated with supersymmetry, Phys. Lett. B 76 (1978) 575, https://doi.org/10.1016/0370-2693(78)90858-4.

[12] G. Jungman, M. Kamionkowski, K. Griest, Supersymmetric dark matter, Phys. Rep. 267 (1996) 195, https://doi.org/10.1016/0370-1573(95)00058-5, arXiv:hep-ph/9506380.

[13] E. Lyndon, B. Philip, LHC machine, J. Instrum. 3 (2008) S08001, https://doi.org/10.1088/1748-0221/3/08/S08001.

[14] J. Alwall, P.C. Schuster, N. Toro, Simplified models for a first characterization of new physics at the LHC, Phys. Rev. D 79 (2009), https://doi.org/10.1103/PhysRevD.79.075020, arXiv:0810.3921.

[15] J. Alwall, M.-P. Le, M. Lisanti, J.G. Wacker, Model-independent jets plus missing energy searches, Phys. Rev. D 79 (2009), https://doi.org/10.1103/PhysRevD.79.015005, arXiv:0809.3264.

[16] LHC New Physics Working Group, D. Alves, et al., Simplified models for LHC new physics searches, J. Phys. G 39 (2012) 105005, https://doi.org/10.1088/0954-3899/39/10/105005, arXiv:1105.2838.

[17] CMS Collaboration, Searches for pair production of third-generation squarks in $\sqrt{s} = 13$ TeV pp collisions, Eur. Phys. J. C 77 (2017) 327, https://doi.org/10.1140/epjc/s10052-017-4853-2, arXiv:1612.03877.

[18] ATLAS Collaboration, Search for a supersymmetric partner to the top quark in final states with jets and missing transverse momentum at $\sqrt{s} = 7$ TeV with the ATLAS detector, Phys. Rev. Lett. 109 (2012) 211802, https://doi.org/10.1103/PhysRevLett.109.211802, arXiv:1208.1447.

[19] ATLAS Collaboration, Search for direct top squark pair production in final states with one isolated lepton, jets, and missing transverse momentum in $\sqrt{s} = 7$ TeV pp collisions using 4.7 fb^{-1} of ATLAS data, Phys. Rev. Lett. 109 (2012) 211803, https://doi.org/10.1103/PhysRevLett.109.211803, arXiv:1208.2590.

[20] ATLAS Collaboration, Search for a heavy top-quark partner in final states with two leptons with the ATLAS detector at the LHC, J. High Energy Phys. 11 (2012) 094, https://doi.org/10.1007/JHEP11(2012)094, arXiv:1209.4186.

[21] ATLAS Collaboration, Search for direct top-squark pair production in final states with two leptons in pp collisions at $\sqrt{s} = 8$ TeV with the ATLAS detector, J. High Energy Phys. 06 (2014) 124, https://doi.org/10.1007/JHEP06(2014)124, arXiv:1403.4853.

[22] ATLAS Collaboration, Search for direct third-generation squark pair production in final states with missing transverse momentum and two b-jets in $\sqrt{s} = 8$ TeV pp collisions with the ATLAS detector, J. High Energy Phys. 10 (2013) 189, https://doi.org/10.1007/JHEP10(2013)189, arXiv:1308.2631.

[23] ATLAS Collaboration, Measurement of spin correlation in top–antitop quark events and search for top squark pair production in pp collisions at $\sqrt{s} = 8$ TeV using the ATLAS detector, Phys. Rev. Lett. 114 (2015) 142001, https://doi.org/10.1103/PhysRevLett.114.142001, arXiv:1412.4742.

[24] ATLAS Collaboration, Search for pair-produced third-generation squarks decaying via charm quarks or in compressed supersymmetric scenarios in pp collisions at $\sqrt{s} = 8$ TeV with the ATLAS detector, Phys. Rev. D 90 (2014) 052008, https://doi.org/10.1103/PhysRevD.90.052008, arXiv:1407.0608.

[25] ATLAS Collaboration, ATLAS Run 1 searches for direct pair production of third-generation squarks at the Large Hadron Collider, Eur. Phys. J. C 75 (2015) 510, https://doi.org/10.1140/epjc/s10052-015-3726-9, arXiv:1506.08616.

[26] CMS Collaboration, Search for top-squark pair production in the single-lepton final state in pp collisions at $\sqrt{s} = 8$ TeV, Eur. Phys. J. C 73 (2013) 2677, https://doi.org/10.1140/epjc/s10052-013-2677-2, arXiv:1308.1586.

[27] CMS Collaboration, Search for supersymmetry in hadronic final states with missing transverse energy using the variables α_T and b-quark multiplicity in pp collisions at $\sqrt{s} = 8$ TeV, Eur. Phys. J. C 73 (2013) 2568, https://doi.org/10.1140/epjc/s10052-013-2568-6, arXiv:1303.2985.

[28] CMS Collaboration, Search for supersymmetry using razor variables in events with b-tagged jets in pp collisions at $\sqrt{s} = 8$ TeV, Phys. Rev. D 91 (2015) 052018, https://doi.org/10.1103/PhysRevD.91.052018, arXiv:1502.00300.

[29] CMS Collaboration, Searches for third-generation squark production in fully hadronic final states in proton–proton collisions at $\sqrt{s} = 8$ TeV, J. High Energy Phys. 06 (2015) 116, https://doi.org/10.1007/JHEP06(2015)116, arXiv:1503.08037.

[30] CMS Collaboration, Search for direct pair production of supersymmetric top quarks decaying to all-hadronic final states in pp collisions at $\sqrt{s} = 8$ TeV, Eur. Phys. J. C 76 (2016) 460, https://doi.org/10.1140/epjc/s10052-016-4292-5, arXiv:1603.00765.

[31] CMS Collaboration, Search for supersymmetry in the multijet and missing transverse momentum final state in pp collisions at 13 TeV, Phys. Lett. B 758 (2016) 152, https://doi.org/10.1016/j.physletb.2016.05.002, arXiv:1602.06581.

[32] CMS Collaboration, Search for new physics with the M_{T2} variable in all-jets final states produced in pp collisions at $\sqrt{s} = 13$ TeV, J. High Energy Phys. 10 (2016) 006, https://doi.org/10.1007/JHEP10(2016)006, arXiv:1603.04053.

[33] CMS Collaboration, Inclusive search for supersymmetry using razor variables in pp collisions at $\sqrt{s} = 13$ TeV, Phys. Rev. D 95 (2017) 012003, https://doi.org/10.1103/PhysRevD.95.012003, arXiv:1609.07658.

[34] CMS Collaboration, A search for new phenomena in pp collisions at $\sqrt{s} = 13$ TeV in final states with missing transverse momentum and at least one jet using the α_T variable, Eur. Phys. J. C 77 (2017) 294, https://doi.org/10.1140/epjc/s10052-017-4787-8, arXiv:1611.00338.

[35] CMS Collaboration, Search for supersymmetry in multijet events with missing transverse momentum in proton–proton collisions at 13 TeV, Phys. Rev. D 96 (2017) 032003, https://dx.doi.org/10.1103/PhysRevD.96.032003, arXiv:1704.07781.

[36] ATLAS Collaboration, Search for new phenomena in final states with an energetic jet and large missing transverse momentum in pp collisions at $\sqrt{s} = 13$ TeV using the ATLAS detector, Phys. Rev. D 94 (2016) 032005, https://doi.org/10.1103/PhysRevD.94.032005, arXiv:1604.07773.

[37] ATLAS Collaboration, Search for Bottom Squark Pair Production in Proton–Proton Collisions at $\sqrt{s} = 13$ TeV with the ATLAS Detector, Technical Report 10, 2016, https://doi.org/10.1140/epjc/s10052-016-4382-4, arXiv:1606.08772.

[38] ATLAS Collaboration, Search for squarks and gluinos in final states with jets and missing transverse momentum at $\sqrt{s} = 13$ TeV with the ATLAS detector, Eur. Phys. J. C 76 (2016) 392, https://doi.org/10.1140/epjc/s10052-016-4184-8, arXiv:1605.03814.

[39] T. Aaltonen, et al., CDF Collaboration, Search for 3- and 4-body decays of the scalar top quark in pp̄ collisions at $\sqrt{s} = 1.8$ TeV, Phys. Lett. B 581 (2004) 147, https://doi.org/10.1016/j.physletb.2003.12.001.

[40] T. Aaltonen, et al., CDF Collaboration, Search for the supersymmetric partner of the top quark in pp̄ collisions at $\sqrt{s} = 1.96$ TeV, Phys. Rev. D 82 (2010) 092001, https://doi.org/10.1103/PhysRevD.82.092001, arXiv:1009.0266.

[41] V.M. Abazov, et al., D0 Collaboration, Search for the lightest scalar top quark in events with two leptons in pp̄ collisions at $\sqrt{s} = 1.96$ TeV, Phys. Lett. B 659 (2008) 500, https://doi.org/10.1016/j.physletb.2007.11.086, arXiv:0707.2864.

[42] V.M. Abazov, et al., D0 Collaboration, Search for pair production of the scalar top quark in muon+tau final states, Phys. Lett. B 710 (2012) 578, https://doi.org/10.1016/j.physletb.2012.03.028, arXiv:1202.1978.

[43] CMS Collaboration, The CMS trigger system, J. Instrum. 12 (2017) P01020, https://doi.org/10.1088/1748-0221/12/01/P01020, arXiv:1609.02366.

[44] CMS Collaboration, The CMS experiment at the CERN LHC, J. Instrum. 3 (2008) S08004, https://doi.org/10.1088/1748-0221/3/08/S08004.

[45] CMS Collaboration, Particle-flow reconstruction and global event description with the CMS detector, J. Instrum. 12 (2017) P10003, https://dx.doi.org/10.1088/1748-0221/12/10/P10003, arXiv:1706.04965.

[46] M. Cacciari, G.P. Salam, G. Soyez, The anti-k_t jet clustering algorithm, J. High Energy Phys. 04 (2008) 063, https://doi.org/10.1088/1126-6708/2008/04/063, arXiv:0802.1189.

[47] M. Cacciari, G.P. Salam, G. Soyez, FastJet user manual, Eur. Phys. J. C 72 (2012) 1896, https://doi.org/10.1140/epjc/s10052-012-1896-2, arXiv:1111.6097.

[48] M. Cacciari, G.P. Salam, Pileup subtraction using jet areas, Phys. Lett. B 659 (2007) 119, https://doi.org/10.1016/j.physletb.2007.09.077, arXiv:0707.1378.

[49] CMS Collaboration, Jet energy scale and resolution in the CMS experiment in pp collisions at 8 TeV, J. Instrum. 12 (2017) P02014, https://doi.org/10.1088/1748-0221/12/02/P02014, arXiv:1607.03663.

[50] CMS Collaboration, Performance of the CMS missing transverse momentum reconstruction in pp data at $\sqrt{s} = 8$ TeV, J. Instrum. 10 (2015) P02006, https://doi.org/10.1088/1748-0221/10/02/P02006, arXiv:1411.0511.

[51] CMS Collaboration, Performance of CMS muon reconstruction in pp collision events at $\sqrt{s} = 7$ TeV, J. Instrum. 7 (2012) P10002, https://doi.org/10.1088/1748-0221/7/10/P10002, arXiv:1206.4071.

[52] CMS Collaboration, Performance of electron reconstruction and selection with the CMS detector in proton–proton collisions at $\sqrt{s} = 8$ TeV, J. Instrum. 10 (2015) P06005, https://doi.org/10.1088/1748-0221/10/06/P06005, arXiv:1502.02701.

[53] CMS Collaboration, Study of Pileup Removal Algorithms for Jet, CMS Physics Analysis Summary CMS-PAS-JME-14-001, 2014, https://cds.cern.ch/record/1751454.

[54] CMS Collaboration, Identification of b-quark jets with the CMS experiment, J. Instrum. 8 (2013) P04013, https://doi.org/10.1088/1748-0221/8/04/P04013, arXiv:1211.4462.

[55] CMS Collaboration, Identification of b Quark Jets at the CMS Experiment in the LHC Run 2, CMS Physics Analysis Summary CMS-PAS-BTV-15-001, 2016, https://cds.cern.ch/record/2138504.

[56] CMS Collaboration, Identification of c-Quark Jets at the CMS Experiment, CMS Physics Analysis Summary CMS-PAS-BTV-16-001, 2016, http://cds.cern.ch/record/2205149.

[57] CMS Collaboration, Measurement of BB̄ angular correlations based on secondary vertex reconstruction at $\sqrt{s} = 7$ TeV, J. High Energy Phys. 03 (2011) 136, https://doi.org/10.1007/JHEP03(2011)136, arXiv:1102.3194.

[58] CMS Collaboration, Search for direct production of supersymmetric partners of the top quark in the all-jets final state in proton–proton collisions at $\sqrt{s} = 13$ TeV, J. High Energy Phys. 10 (2017) 005, https://dx.doi.org/10.1007/JHEP10(2017)005, arXiv:1707.03316.

[59] J. Alwall, R. Frederix, S. Frixione, V. Hirschi, F. Maltoni, O. Mattelaer, H.S. Shao, T. Stelzer, P. Torrielli, M. Zaro, The automated computation of tree-level and next-to-leading order differential cross sections, and their matching to parton shower simulations, J. High Energy Phys. 07 (2014) 079, https://doi.org/10.1007/JHEP07(2014)079, arXiv:1405.0301.

[60] R.D. Ball, et al., NNPDF Collaboration, Parton distributions for the LHC Run II, J. High Energy Phys. 04 (2015) 040, https://doi.org/10.1007/JHEP04(2015)040, arXiv:1410.8849.

[61] P. Nason, A new method for combining NLO QCD with shower Monte Carlo algorithms, J. High Energy Phys. 11 (2004) 040, https://doi.org/10.1088/1126-6708/2004/11/040, arXiv:hep-ph/0409146.

[62] S. Frixione, P. Nason, C. Oleari, Matching NLO QCD computations with parton shower simulations: the POWHEG method, J. High Energy Phys. 11 (2007) 070, https://doi.org/10.1088/1126-6708/2007/11/070, arXiv:0709.2092.

[63] S. Alioli, P. Nason, C. Oleari, E. Re, A general framework for implementing NLO calculations in shower Monte Carlo programs: the POWHEG BOX, J. High Energy Phys. 06 (2010) 043, https://doi.org/10.1007/JHEP06(2010)043, arXiv:1002.2581.

[64] E. Re, Single-top Wt-channel production matched with parton showers using the POWHEG method, Eur. Phys. J. C 71 (2011) 1547, https://doi.org/10.1140/epjc/s10052-011-1547-z, arXiv:1009.2450.

[65] T. Sjöstrand, S. Ask, J.R. Christiansen, R. Corke, N. Desai, P. Ilten, S. Mrenna, S. Prestel, C.O. Rasmussen, P.Z. Skands, An introduction to PYTHIA 8.2, Comput. Phys. Commun. 191 (2015) 159, https://doi.org/10.1016/j.cpc.2015.01.024, arXiv:1410.3012.

[66] S. Agostinelli, et al., GEANT4 Collaboration, GEANT4—a simulation toolkit, Nucl. Instrum. Methods Phys. Res., Sect. A 506 (2003) 250, https://doi.org/10.1016/S0168-9002(03)01368-8.

[67] S. Abdullin, P. Azzi, F. Beaudette, P. Janot, A. Perrotta, The fast simulation of the CMS detector at LHC, J. Phys. Conf. Ser. 331 (2011) 032049, https://doi.org/10.1088/1742-6596/331/3/032049.

[68] C. Borschensky, M. Krämer, A. Kulesza, M. Mangano, S. Padhi, T. Plehn, X. Portell, Squark and gluino production cross sections in pp collisions at $\sqrt{s} =$ 13, 14, 33 and 100 TeV, Eur. Phys. J. C 74 (2014) 3174, https://doi.org/10.1140/epjc/s10052-014-3174-y, arXiv:1407.5066.

[69] D.R. Tovey, On measuring the masses of pair-produced semi-invisibly decaying particles at hadron colliders, J. High Energy Phys. 04 (2008) 034, https://doi.org/10.1088/1126-6708/2008/04/034, arXiv:0802.2879.

[70] G. Polesello, D.R. Tovey, Supersymmetric particle mass measurement with the boost-corrected contransverse mass, J. High Energy Phys. 03 (2010) 030, https://doi.org/10.1007/JHEP03(2010)030, arXiv:0910.0174.

[71] Particle Data Group, C. Patrignani, et al., Review of particle physics, Chin. Phys. C 40 (2016) 100001, https://doi.org/10.1088/1674-1137/40/10/100001.

[72] CMS Collaboration, CMS Luminosity Measurements for the 2016 Data Taking Period, CMS Physics Analysis Summary CMS-PAS-LUM-17-001, 2017, https://cds.cern.ch/record/2257069.

[73] T. Junk, Confidence level computation for combining searches with small statistics, Nucl. Instrum. Methods Phys. Res., Sect. A 434 (1999) 435, https://doi.org/10.1016/S0168-9002(99)00498-2, arXiv:hep-ex/9902006.

[74] A.L. Read, Presentation of search results: the CLs technique, J. Phys. G 28 (2002) 2693, https://doi.org/10.1088/0954-3899/28/10/313.

[75] ATLAS and CMS Collaborations, Procedure for the LHC Higgs Boson Search Combination in Summer 2011, Technical Report ATL-PHYS-PUB-2011-11, CMS-NOTE-2011-005, 2011, http://cdsweb.cern.ch/record/1379837.

[76] G. Cowan, K. Cranmer, E. Gross, O. Vitells, Asymptotic formulae for likelihood-based tests of new physics, Eur. Phys. J. C 71 (2011) 1554, https://doi.org/10.1140/epjc/s10052-011-1554-0, arXiv:1007.1727, Erratum: https://doi.org/10.1140/epjc/s10052-013-2501-z.

[77] CMS Collaboration, Simplified Likelihood for the Re-Interpretation of Public CMS Results, Technical Report CERN-CMS-NOTE-2017-001, 2017, http://cds.cern.ch/record/2242860.

The CMS Collaboration

A.M. Sirunyan, A. Tumasyan

Yerevan Physics Institute, Yerevan, Armenia

W. Adam, F. Ambrogi, E. Asilar, T. Bergauer, J. Brandstetter, E. Brondolin, M. Dragicevic, J. Erö, M. Flechl, M. Friedl, R. Frühwirth [1], V.M. Ghete, J. Grossmann, J. Hrubec, M. Jeitler [1], A. König, N. Krammer, I. Krätschmer, D. Liko, T. Madlener, I. Mikulec, E. Pree, D. Rabady, N. Rad, H. Rohringer, J. Schieck [1], R. Schöfbeck, M. Spanring, D. Spitzbart, J. Strauss, W. Waltenberger, J. Wittmann, C.-E. Wulz [1], M. Zarucki

Institut für Hochenergiephysik, Wien, Austria

V. Chekhovsky, J. Suarez Gonzalez

Institute for Nuclear Problems, Minsk, Belarus

E.A. De Wolf, D. Di Croce, X. Janssen, J. Lauwers, H. Van Haevermaet, P. Van Mechelen, N. Van Remortel

Universiteit Antwerpen, Antwerpen, Belgium

S. Abu Zeid, F. Blekman, J. D'Hondt, I. De Bruyn, J. De Clercq, K. Deroover, G. Flouris, D. Lontkovskyi, S. Lowette, S. Moortgat, L. Moreels, A. Olbrechts, Q. Python, K. Skovpen, S. Tavernier, W. Van Doninck, P. Van Mulders, I. Van Parijs

Vrije Universiteit Brussel, Brussel, Belgium

H. Brun, B. Clerbaux, G. De Lentdecker, H. Delannoy, G. Fasanella, L. Favart, R. Goldouzian, A. Grebenyuk, G. Karapostoli, T. Lenzi, J. Luetic, T. Maerschalk, A. Marinov, A. Randle-conde, T. Seva, C. Vander Velde, P. Vanlaer, D. Vannerom, R. Yonamine, F. Zenoni, F. Zhang [2]

Université Libre de Bruxelles, Bruxelles, Belgium

A. Cimmino, T. Cornelis, D. Dobur, A. Fagot, M. Gul, I. Khvastunov, D. Poyraz, C. Roskas, S. Salva, M. Tytgat, W. Verbeke, N. Zaganidis

Ghent University, Ghent, Belgium

H. Bakhshiansohi, O. Bondu, S. Brochet, G. Bruno, A. Caudron, S. De Visscher, C. Delaere, M. Delcourt, B. Francois, A. Giammanco, A. Jafari, M. Komm, G. Krintiras, V. Lemaitre, A. Magitteri, A. Mertens, M. Musich, K. Piotrzkowski, L. Quertenmont, M. Vidal Marono, S. Wertz

Université Catholique de Louvain, Louvain-la-Neuve, Belgium

N. Beliy

Université de Mons, Mons, Belgium

W.L. Aldá Júnior, F.L. Alves, G.A. Alves, L. Brito, M. Correa Martins Junior, C. Hensel, A. Moraes, M.E. Pol, P. Rebello Teles

Centro Brasileiro de Pesquisas Fisicas, Rio de Janeiro, Brazil

E. Belchior Batista Das Chagas, W. Carvalho, J. Chinellato [3], A. Custódio, E.M. Da Costa, G.G. Da Silveira [4], D. De Jesus Damiao, S. Fonseca De Souza, L.M. Huertas Guativa, H. Malbouisson, M. Melo De Almeida, C. Mora Herrera, L. Mundim, H. Nogima, A. Santoro, A. Sznajder, E.J. Tonelli Manganote [3], F. Torres Da Silva De Araujo, A. Vilela Pereira

Universidade do Estado do Rio de Janeiro, Rio de Janeiro, Brazil

S. Ahuja [a], C.A. Bernardes [a], T.R. Fernandez Perez Tomei [a], E.M. Gregores [b], P.G. Mercadante [b], S.F. Novaes [a], Sandra S. Padula [a], D. Romero Abad [b], J.C. Ruiz Vargas [a]

[a] *Universidade Estadual Paulista, São Paulo, Brazil*
[b] *Universidade Federal do ABC, São Paulo, Brazil*

A. Aleksandrov, R. Hadjiiska, P. Iaydjiev, M. Misheva, M. Rodozov, M. Shopova, S. Stoykova, G. Sultanov

Institute for Nuclear Research and Nuclear Energy of Bulgaria Academy of Sciences, Bulgaria

A. Dimitrov, I. Glushkov, L. Litov, B. Pavlov, P. Petkov

University of Sofia, Sofia, Bulgaria

W. Fang [5], X. Gao [5]

Beihang University, Beijing, China

M. Ahmad, J.G. Bian, G.M. Chen, H.S. Chen, M. Chen, Y. Chen, C.H. Jiang, D. Leggat, H. Liao, Z. Liu, F. Romeo, S.M. Shaheen, A. Spiezia, J. Tao, C. Wang, Z. Wang, E. Yazgan, H. Zhang, J. Zhao

Institute of High Energy Physics, Beijing, China

Y. Ban, G. Chen, Q. Li, S. Liu, Y. Mao, S.J. Qian, D. Wang, Z. Xu

State Key Laboratory of Nuclear Physics and Technology, Peking University, Beijing, China

C. Avila, A. Cabrera, L.F. Chaparro Sierra, C. Florez, C.F. González Hernández, J.D. Ruiz Alvarez

Universidad de Los Andes, Bogota, Colombia

B. Courbon, N. Godinovic, D. Lelas, I. Puljak, P.M. Ribeiro Cipriano, T. Sculac

University of Split, Faculty of Electrical Engineering, Mechanical Engineering and Naval Architecture, Split, Croatia

Z. Antunovic, M. Kovac

University of Split, Faculty of Science, Split, Croatia

V. Brigljevic, D. Ferencek, K. Kadija, B. Mesic, A. Starodumov [6], T. Susa

Institute Rudjer Boskovic, Zagreb, Croatia

M.W. Ather, A. Attikis, G. Mavromanolakis, J. Mousa, C. Nicolaou, F. Ptochos, P.A. Razis, H. Rykaczewski

University of Cyprus, Nicosia, Cyprus

M. Finger [7], M. Finger Jr. [7]

Charles University, Prague, Czech Republic

E. Carrera Jarrin

Universidad San Francisco de Quito, Quito, Ecuador

A.A. Abdelalim [8,9], Y. Mohammed [10], E. Salama [11,12]

Academy of Scientific Research and Technology of the Arab Republic of Egypt, Egyptian Network of High Energy Physics, Cairo, Egypt

R.K. Dewanjee, M. Kadastik, L. Perrini, M. Raidal, A. Tiko, C. Veelken

National Institute of Chemical Physics and Biophysics, Tallinn, Estonia

P. Eerola, J. Pekkanen, M. Voutilainen

Department of Physics, University of Helsinki, Helsinki, Finland

J. Härkönen, T. Järvinen, V. Karimäki, R. Kinnunen, T. Lampén, K. Lassila-Perini, S. Lehti, T. Lindén,
P. Luukka, E. Tuominen, J. Tuominiemi, E. Tuovinen

Helsinki Institute of Physics, Helsinki, Finland

J. Talvitie, T. Tuuva

Lappeenranta University of Technology, Lappeenranta, Finland

M. Besancon, F. Couderc, M. Dejardin, D. Denegri, J.L. Faure, F. Ferri, S. Ganjour, S. Ghosh, A. Givernaud,
P. Gras, G. Hamel de Monchenault, P. Jarry, I. Kucher, E. Locci, M. Machet, J. Malcles, G. Negro, J. Rander,
A. Rosowsky, M.Ö. Sahin, M. Titov

IRFU, CEA, Université Paris-Saclay, Gif-sur-Yvette, France

A. Abdulsalam, I. Antropov, S. Baffioni, F. Beaudette, P. Busson, L. Cadamuro, C. Charlot,
R. Granier de Cassagnac, M. Jo, S. Lisniak, A. Lobanov, J. Martin Blanco, M. Nguyen, C. Ochando,
G. Ortona, P. Paganini, P. Pigard, S. Regnard, R. Salerno, J.B. Sauvan, Y. Sirois, A.G. Stahl Leiton, T. Strebler,
Y. Yilmaz, A. Zabi, A. Zghiche

Laboratoire Leprince-Ringuet, Ecole polytechnique, CNRS/IN2P3, Université Paris-Saclay, Palaiseau, France

J.-L. Agram [13], J. Andrea, D. Bloch, J.-M. Brom, M. Buttignol, E.C. Chabert, N. Chanon, C. Collard,
E. Conte [13], X. Coubez, J.-C. Fontaine [13], D. Gelé, U. Goerlach, M. Jansová, A.-C. Le Bihan, N. Tonon,
P. Van Hove

Université de Strasbourg, CNRS, IPHC UMR 7178, F-67000 Strasbourg, France

S. Gadrat

Centre de Calcul de l'Institut National de Physique Nucléaire et de Physique des Particules, CNRS/IN2P3, Villeurbanne, France

S. Beauceron, C. Bernet, G. Boudoul, R. Chierici, D. Contardo, P. Depasse, H. El Mamouni, J. Fay, L. Finco,
S. Gascon, M. Gouzevitch, G. Grenier, B. Ille, F. Lagarde, I.B. Laktineh, M. Lethuillier, L. Mirabito,
A.L. Pequegnot, S. Perries, A. Popov [14], V. Sordini, M. Vander Donckt, S. Viret

Université de Lyon, Université Claude Bernard Lyon 1, CNRS-IN2P3, Institut de Physique Nucléaire de Lyon, Villeurbanne, France

T. Toriashvili [15]

Georgian Technical University, Tbilisi, Georgia

D. Lomidze

Tbilisi State University, Tbilisi, Georgia

C. Autermann, S. Beranek, L. Feld, M.K. Kiesel, K. Klein, M. Lipinski, M. Preuten, C. Schomakers, J. Schulz, T. Verlage

RWTH Aachen University, I. Physikalisches Institut, Aachen, Germany

A. Albert, E. Dietz-Laursonn, D. Duchardt, M. Endres, M. Erdmann, S. Erdweg, T. Esch, R. Fischer, A. Güth, M. Hamer, T. Hebbeker, C. Heidemann, K. Hoepfner, S. Knutzen, M. Merschmeyer, A. Meyer, P. Millet, S. Mukherjee, M. Olschewski, K. Padeken, T. Pook, M. Radziej, H. Reithler, M. Rieger, F. Scheuch, D. Teyssier, S. Thüer

RWTH Aachen University, III. Physikalisches Institut A, Aachen, Germany

G. Flügge, B. Kargoll, T. Kress, A. Künsken, J. Lingemann, T. Müller, A. Nehrkorn, A. Nowack, C. Pistone, O. Pooth, A. Stahl [16]

RWTH Aachen University, III. Physikalisches Institut B, Aachen, Germany

M. Aldaya Martin, T. Arndt, C. Asawatangtrakuldee, K. Beernaert, O. Behnke, U. Behrens, A. Bermúdez Martínez, A.A. Bin Anuar, K. Borras [17], V. Botta, A. Campbell, P. Connor, C. Contreras-Campana, F. Costanza, C. Diez Pardos, G. Eckerlin, D. Eckstein, T. Eichhorn, E. Eren, E. Gallo [18], J. Garay Garcia, A. Geiser, A. Gizhko, J.M. Grados Luyando, A. Grohsjean, P. Gunnellini, A. Harb, J. Hauk, M. Hempel [19], H. Jung, A. Kalogeropoulos, M. Kasemann, J. Keaveney, C. Kleinwort, I. Korol, D. Krücker, W. Lange, A. Lelek, T. Lenz, J. Leonard, K. Lipka, W. Lohmann [19], R. Mankel, I.-A. Melzer-Pellmann, A.B. Meyer, G. Mittag, J. Mnich, A. Mussgiller, E. Ntomari, D. Pitzl, R. Placakyte, A. Raspereza, B. Roland, M. Savitskyi, P. Saxena, R. Shevchenko, S. Spannagel, N. Stefaniuk, G.P. Van Onsem, R. Walsh, Y. Wen, K. Wichmann, C. Wissing, O. Zenaiev

Deutsches Elektronen-Synchrotron, Hamburg, Germany

S. Bein, V. Blobel, M. Centis Vignali, A.R. Draeger, T. Dreyer, E. Garutti, D. Gonzalez, J. Haller, A. Hinzmann, M. Hoffmann, A. Karavdina, R. Klanner, R. Kogler, N. Kovalchuk, S. Kurz, T. Lapsien, I. Marchesini, D. Marconi, M. Meyer, M. Niedziela, D. Nowatschin, F. Pantaleo [16], T. Peiffer, A. Perieanu, C. Scharf, P. Schleper, A. Schmidt, S. Schumann, J. Schwandt, J. Sonneveld, H. Stadie, G. Steinbrück, F.M. Stober, M. Stöver, H. Tholen, D. Troendle, E. Usai, L. Vanelderen, A. Vanhoefer, B. Vormwald

University of Hamburg, Hamburg, Germany

M. Akbiyik, C. Barth, S. Baur, E. Butz, R. Caspart, T. Chwalek, F. Colombo, W. De Boer, A. Dierlamm, B. Freund, R. Friese, M. Giffels, A. Gilbert, D. Haitz, F. Hartmann [16], S.M. Heindl, U. Husemann, F. Kassel [16], S. Kudella, H. Mildner, M.U. Mozer, Th. Müller, M. Plagge, G. Quast, K. Rabbertz, M. Schröder, I. Shvetsov, G. Sieber, H.J. Simonis, R. Ulrich, S. Wayand, M. Weber, T. Weiler, S. Williamson, C. Wöhrmann, R. Wolf

Institut für Experimentelle Kernphysik, Karlsruhe, Germany

G. Anagnostou, G. Daskalakis, T. Geralis, V.A. Giakoumopoulou, A. Kyriakis, D. Loukas, I. Topsis-Giotis

Institute of Nuclear and Particle Physics (INPP), NCSR Demokritos, Aghia Paraskevi, Greece

S. Kesisoglou, A. Panagiotou, N. Saoulidou

National and Kapodistrian University of Athens, Athens, Greece

I. Evangelou, C. Foudas, P. Kokkas, S. Mallios, N. Manthos, I. Papadopoulos, E. Paradas, J. Strologas, F.A. Triantis

University of Ioánnina, Ioánnina, Greece

M. Csanad, N. Filipovic, G. Pasztor

MTA-ELTE Lendület CMS Particle and Nuclear Physics Group, Eötvös Loránd University, Budapest, Hungary

G. Bencze, C. Hajdu, D. Horvath [20], Á. Hunyadi, F. Sikler, V. Veszpremi, G. Vesztergombi [21], A.J. Zsigmond

Wigner Research Centre for Physics, Budapest, Hungary

N. Beni, S. Czellar, J. Karancsi [22], A. Makovec, J. Molnar, Z. Szillasi

Institute of Nuclear Research ATOMKI, Debrecen, Hungary

M. Bartók [21], P. Raics, Z.L. Trocsanyi, B. Ujvari

Institute of Physics, University of Debrecen, Debrecen, Hungary

S. Choudhury, J.R. Komaragiri

Indian Institute of Science (IISc), Bangalore, India

S. Bahinipati [23], S. Bhowmik, P. Mal, K. Mandal, A. Nayak [24], D.K. Sahoo [23], N. Sahoo, S.K. Swain

National Institute of Science Education and Research, Bhubaneswar, India

S. Bansal, S.B. Beri, V. Bhatnagar, U. Bhawandeep, R. Chawla, N. Dhingra, A.K. Kalsi, A. Kaur, M. Kaur, R. Kumar, P. Kumari, A. Mehta, J.B. Singh, G. Walia

Panjab University, Chandigarh, India

Ashok Kumar, Aashaq Shah, A. Bhardwaj, S. Chauhan, B.C. Choudhary, R.B. Garg, S. Keshri, A. Kumar, S. Malhotra, M. Naimuddin, K. Ranjan, R. Sharma, V. Sharma

University of Delhi, Delhi, India

R. Bhardwaj, R. Bhattacharya, S. Bhattacharya, S. Dey, S. Dutt, S. Dutta, S. Ghosh, N. Majumdar, A. Modak, K. Mondal, S. Mukhopadhyay, S. Nandan, A. Purohit, A. Roy, D. Roy, S. Roy Chowdhury, S. Sarkar, M. Sharan, S. Thakur

Saha Institute of Nuclear Physics, HBNI, Kolkata, India

P.K. Behera

Indian Institute of Technology Madras, Madras, India

R. Chudasama, D. Dutta, V. Jha, V. Kumar, A.K. Mohanty [16], P.K. Netrakanti, L.M. Pant, P. Shukla, A. Topkar

Bhabha Atomic Research Centre, Mumbai, India

T. Aziz, S. Dugad, B. Mahakud, S. Mitra, G.B. Mohanty, B. Parida, N. Sur, B. Sutar

Tata Institute of Fundamental Research-A, Mumbai, India

S. Banerjee, S. Bhattacharya, S. Chatterjee, P. Das, M. Guchait, Sa. Jain, S. Kumar, M. Maity [25], G. Majumder, K. Mazumdar, T. Sarkar [25], N. Wickramage [26]

Tata Institute of Fundamental Research-B, Mumbai, India

S. Chauhan, S. Dube, V. Hegde, A. Kapoor, K. Kothekar, S. Pandey, A. Rane, S. Sharma

Indian Institute of Science Education and Research (IISER), Pune, India

S. Chenarani [27], E. Eskandari Tadavani, S.M. Etesami [27], M. Khakzad, M. Mohammadi Najafabadi, M. Naseri, S. Paktinat Mehdiabadi [28], F. Rezaei Hosseinabadi, B. Safarzadeh [29], M. Zeinali

Institute for Research in Fundamental Sciences (IPM), Tehran, Iran

M. Felcini, M. Grunewald

University College Dublin, Dublin, Ireland

M. Abbrescia [a,b], C. Calabria [a,b], C. Caputo [a,b], A. Colaleo [a], D. Creanza [a,c], L. Cristella [a,b], N. De Filippis [a,c], M. De Palma [a,b], F. Errico [a,b], L. Fiore [a], G. Iaselli [a,c], S. Lezki [a,b], G. Maggi [a,c], M. Maggi [a], G. Miniello [a,b], S. My [a,b], S. Nuzzo [a,b], A. Pompili [a,b], G. Pugliese [a,c], R. Radogna [a,b], A. Ranieri [a], G. Selvaggi [a,b], A. Sharma [a], L. Silvestris [a,16], R. Venditti [a], P. Verwilligen [a]

[a] *INFN Sezione di Bari, Bari, Italy*
[b] *Università di Bari, Bari, Italy*
[c] *Politecnico di Bari, Bari, Italy*

G. Abbiendi [a], C. Battilana [a,b], D. Bonacorsi [a,b], S. Braibant-Giacomelli [a,b], R. Campanini [a,b], P. Capiluppi [a,b], A. Castro [a,b], F.R. Cavallo [a], S.S. Chhibra [a], G. Codispoti [a,b], M. Cuffiani [a,b], G.M. Dallavalle [a], F. Fabbri [a], A. Fanfani [a,b], D. Fasanella [a,b], P. Giacomelli [a], C. Grandi [a], L. Guiducci [a,b], S. Marcellini [a], G. Masetti [a], A. Montanari [a], F.L. Navarria [a,b], A. Perrotta [a], A.M. Rossi [a,b], T. Rovelli [a,b], G.P. Siroli [a,b], N. Tosi [a]

[a] *INFN Sezione di Bologna, Bologna, Italy*
[b] *Università di Bologna, Bologna, Italy*

S. Albergo [a,b], S. Costa [a,b], A. Di Mattia [a], F. Giordano [a,b], R. Potenza [a,b], A. Tricomi [a,b], C. Tuve [a,b]

[a] *INFN Sezione di Catania, Catania, Italy*
[b] *Università di Catania, Catania, Italy*

G. Barbagli [a], K. Chatterjee [a,b], V. Ciulli [a,b], C. Civinini [a], R. D'Alessandro [a,b], E. Focardi [a,b], P. Lenzi [a,b], M. Meschini [a], S. Paoletti [a], L. Russo [a,30], G. Sguazzoni [a], D. Strom [a], L. Viliani [a,b,16]

[a] *INFN Sezione di Firenze, Firenze, Italy*
[b] *Università di Firenze, Firenze, Italy*

L. Benussi, S. Bianco, F. Fabbri, D. Piccolo, F. Primavera [16]

INFN Laboratori Nazionali di Frascati, Frascati, Italy

V. Calvelli [a,b], F. Ferro [a], E. Robutti [a], S. Tosi [a,b]

[a] *INFN Sezione di Genova, Genova, Italy*
[b] *Università di Genova, Genova, Italy*

L. Brianza [a,b], F. Brivio [a,b], V. Ciriolo [a,b], M.E. Dinardo [a,b], S. Fiorendi [a,b], S. Gennai [a], A. Ghezzi [a,b], P. Govoni [a,b], M. Malberti [a,b], S. Malvezzi [a], R.A. Manzoni [a,b], D. Menasce [a], L. Moroni [a], M. Paganoni [a,b], K. Pauwels [a,b], D. Pedrini [a], S. Pigazzini [a,b,31], S. Ragazzi [a,b], T. Tabarelli de Fatis [a,b]

[a] *INFN Sezione di Milano-Bicocca, Milano, Italy*
[b] *Università di Milano-Bicocca, Milano, Italy*

S. Buontempo [a], N. Cavallo [a,c], S. Di Guida [a,d,16], F. Fabozzi [a,c], F. Fienga [a,b], A.O.M. Iorio [a,b], W.A. Khan [a], L. Lista [a], S. Meola [a,d,16], P. Paolucci [a,16], C. Sciacca [a,b], F. Thyssen [a]

[a] *INFN Sezione di Napoli, Napoli, Italy*
[b] *Università di Napoli 'Federico II', Napoli, Italy*
[c] *Università della Basilicata, Potenza, Italy*
[d] *Università G. Marconi, Roma, Italy*

P. Azzi [a,16], N. Bacchetta [a], L. Benato [a,b], D. Bisello [a,b], A. Boletti [a,b], R. Carlin [a,b], A. Carvalho Antunes De Oliveira [a,b], P. Checchia [a], M. Dall'Osso [a,b], P. De Castro Manzano [a], T. Dorigo [a], U. Dosselli [a], F. Gasparini [a,b], U. Gasparini [a,b], A. Gozzelino [a], S. Lacaprara [a], M. Margoni [a,b], A.T. Meneguzzo [a,b], N. Pozzobon [a,b], P. Ronchese [a,b], R. Rossin [a,b], F. Simonetto [a,b], E. Torassa [a], M. Zanetti [a,b], P. Zotto [a,b], G. Zumerle [a,b]

[a] *INFN Sezione di Padova, Padova, Italy*
[b] *Università di Padova, Padova, Italy*
[c] *Università di Trento, Trento, Italy*

A. Braghieri [a], F. Fallavollita [a,b], A. Magnani [a,b], P. Montagna [a,b], S.P. Ratti [a,b], V. Re [a], M. Ressegotti, C. Riccardi [a,b], P. Salvini [a], I. Vai [a,b], P. Vitulo [a,b]

[a] *INFN Sezione di Pavia, Pavia, Italy*
[b] *Università di Pavia, Pavia, Italy*

L. Alunni Solestizi [a,b], M. Biasini [a,b], G.M. Bilei [a], C. Cecchi [a,b], D. Ciangottini [a,b], L. Fanò [a,b], P. Lariccia [a,b], R. Leonardi [a,b], E. Manoni [a], G. Mantovani [a,b], V. Mariani [a,b], M. Menichelli [a], A. Rossi [a,b], A. Santocchia [a,b], D. Spiga [a]

[a] *INFN Sezione di Perugia, Perugia, Italy*
[b] *Università di Perugia, Perugia, Italy*

K. Androsov [a], P. Azzurri [a,16], G. Bagliesi [a], J. Bernardini [a], T. Boccali [a], L. Borrello, R. Castaldi [a], M.A. Ciocci [a,b], R. Dell'Orso [a], G. Fedi [a], L. Giannini [a,c], A. Giassi [a], M.T. Grippo [a,30], F. Ligabue [a,c], T. Lomtadze [a], E. Manca [a,c], G. Mandorli [a,c], L. Martini [a,b], A. Messineo [a,b], F. Palla [a], A. Rizzi [a,b], A. Savoy-Navarro [a,32], P. Spagnolo [a], R. Tenchini [a], G. Tonelli [a,b], A. Venturi [a], P.G. Verdini [a]

[a] *INFN Sezione di Pisa, Pisa, Italy*
[b] *Università di Pisa, Pisa, Italy*
[c] *Scuola Normale Superiore di Pisa, Pisa, Italy*

L. Barone [a,b], F. Cavallari [a], M. Cipriani [a,b], D. Del Re [a,b,16], M. Diemoz [a], S. Gelli [a,b], E. Longo [a,b], F. Margaroli [a,b], B. Marzocchi [a,b], P. Meridiani [a], G. Organtini [a,b], R. Paramatti [a,b], F. Preiato [a,b], S. Rahatlou [a,b], C. Rovelli [a], F. Santanastasio [a,b]

[a] *INFN Sezione di Roma, Rome, Italy*
[b] *Sapienza Università di Roma, Rome, Italy*

N. Amapane [a,b], R. Arcidiacono [a,c], S. Argiro [a,b], M. Arneodo [a,c], N. Bartosik [a], R. Bellan [a,b], C. Biino [a], N. Cartiglia [a], F. Cenna [a,b], M. Costa [a,b], R. Covarelli [a,b], A. Degano [a,b], N. Demaria [a], B. Kiani [a,b], C. Mariotti [a], S. Maselli [a], E. Migliore [a,b], V. Monaco [a,b], E. Monteil [a,b], M. Monteno [a], M.M. Obertino [a,b], L. Pacher [a,b], N. Pastrone [a], M. Pelliccioni [a], G.L. Pinna Angioni [a,b], F. Ravera [a,b], A. Romero [a,b], M. Ruspa [a,c], R. Sacchi [a,b], K. Shchelina [a,b], V. Sola [a], A. Solano [a,b], A. Staiano [a], P. Traczyk [a,b]

[a] *INFN Sezione di Torino, Torino, Italy*
[b] *Università di Torino, Torino, Italy*
[c] *Università del Piemonte Orientale, Novara, Italy*

S. Belforte [a], M. Casarsa [a], F. Cossutti [a], G. Della Ricca [a,b], A. Zanetti [a]

[a] *INFN Sezione di Trieste, Trieste, Italy*
[b] *Università di Trieste, Trieste, Italy*

D.H. Kim, G.N. Kim, M.S. Kim, J. Lee, S. Lee, S.W. Lee, C.S. Moon, Y.D. Oh, S. Sekmen, D.C. Son, Y.C. Yang

Kyungpook National University, Daegu, Republic of Korea

A. Lee

Chonbuk National University, Jeonju, Republic of Korea

H. Kim, D.H. Moon, G. Oh

Chonnam National University, Institute for Universe and Elementary Particles, Kwangju, Republic of Korea

J.A. Brochero Cifuentes, J. Goh, T.J. Kim

Hanyang University, Seoul, Republic of Korea

S. Cho, S. Choi, Y. Go, D. Gyun, S. Ha, B. Hong, Y. Jo, Y. Kim, K. Lee, K.S. Lee, S. Lee, J. Lim, S.K. Park, Y. Roh

Korea University, Seoul, Republic of Korea

J. Almond, J. Kim, J.S. Kim, H. Lee, K. Lee, K. Nam, S.B. Oh, B.C. Radburn-Smith, S.h. Seo, U.K. Yang, H.D. Yoo, G.B. Yu

Seoul National University, Seoul, Republic of Korea

M. Choi, H. Kim, J.H. Kim, J.S.H. Lee, I.C. Park, G. Ryu

University of Seoul, Seoul, Republic of Korea

Y. Choi, C. Hwang, J. Lee, I. Yu

Sungkyunkwan University, Suwon, Republic of Korea

V. Dudenas, A. Juodagalvis, J. Vaitkus

Vilnius University, Vilnius, Lithuania

I. Ahmed, Z.A. Ibrahim, M.A.B. Md Ali [33], F. Mohamad Idris [34], W.A.T. Wan Abdullah, M.N. Yusli, Z. Zolkapli

National Centre for Particle Physics, Universiti Malaya, Kuala Lumpur, Malaysia

H. Castilla-Valdez, E. De La Cruz-Burelo, I. Heredia-De La Cruz [35], R. Lopez-Fernandez, J. Mejia Guisao, A. Sanchez-Hernandez

Centro de Investigacion y de Estudios Avanzados del IPN, Mexico City, Mexico

S. Carrillo Moreno, C. Oropeza Barrera, F. Vazquez Valencia

Universidad Iberoamericana, Mexico City, Mexico

I. Pedraza, H.A. Salazar Ibarguen, C. Uribe Estrada

Benemerita Universidad Autonoma de Puebla, Puebla, Mexico

A. Morelos Pineda

Universidad Autónoma de San Luis Potosí, San Luis Potosí, Mexico

D. Krofcheck

University of Auckland, Auckland, New Zealand

P.H. Butler

University of Canterbury, Christchurch, New Zealand

A. Ahmad, M. Ahmad, Q. Hassan, H.R. Hoorani, A. Saddique, M.A. Shah, M. Shoaib, M. Waqas

National Centre for Physics, Quaid-I-Azam University, Islamabad, Pakistan

H. Bialkowska, M. Bluj, B. Boimska, T. Frueboes, M. Górski, M. Kazana, K. Nawrocki, K. Romanowska-Rybinska, M. Szleper, P. Zalewski

National Centre for Nuclear Research, Swierk, Poland

K. Bunkowski, A. Byszuk [36], K. Doroba, A. Kalinowski, M. Konecki, J. Krolikowski, M. Misiura, M. Olszewski, A. Pyskir, M. Walczak

Institute of Experimental Physics, Faculty of Physics, University of Warsaw, Warsaw, Poland

P. Bargassa, C. Beirão Da Cruz E Silva, B. Calpas, A. Di Francesco, P. Faccioli, M. Gallinaro, J. Hollar, N. Leonardo, L. Lloret Iglesias, M.V. Nemallapudi, J. Seixas, O. Toldaiev, D. Vadruccio, J. Varela

Laboratório de Instrumentação e Física Experimental de Partículas, Lisboa, Portugal

S. Afanasiev, P. Bunin, M. Gavrilenko, I. Golutvin, I. Gorbunov, A. Kamenev, V. Karjavin, A. Lanev, A. Malakhov, V. Matveev [37,38], V. Palichik, V. Perelygin, S. Shmatov, S. Shulha, N. Skatchkov, V. Smirnov, N. Voytishin, A. Zarubin

Joint Institute for Nuclear Research, Dubna, Russia

Y. Ivanov, V. Kim [39], E. Kuznetsova [40], P. Levchenko, V. Murzin, V. Oreshkin, I. Smirnov, V. Sulimov, L. Uvarov, S. Vavilov, A. Vorobyev

Petersburg Nuclear Physics Institute, Gatchina (St. Petersburg), Russia

Yu. Andreev, A. Dermenev, S. Gninenko, N. Golubev, A. Karneyeu, M. Kirsanov, N. Krasnikov, A. Pashenkov, D. Tlisov, A. Toropin

Institute for Nuclear Research, Moscow, Russia

V. Epshteyn, V. Gavrilov, N. Lychkovskaya, V. Popov, I. Pozdnyakov, G. Safronov, A. Spiridonov, A. Stepennov, M. Toms, E. Vlasov, A. Zhokin

Institute for Theoretical and Experimental Physics, Moscow, Russia

T. Aushev, A. Bylinkin [38]

Moscow Institute of Physics and Technology, Moscow, Russia

R. Chistov [41], M. Danilov [41], P. Parygin, D. Philippov, S. Polikarpov, E. Tarkovskii

National Research Nuclear University 'Moscow Engineering Physics Institute' (MEPhI), Moscow, Russia

V. Andreev, M. Azarkin [38], I. Dremin [38], M. Kirakosyan [38], A. Terkulov

P.N. Lebedev Physical Institute, Moscow, Russia

A. Baskakov, A. Belyaev, E. Boos, M. Dubinin [42], L. Dudko, A. Ershov, A. Gribushin, V. Klyukhin, O. Kodolova, I. Lokhtin, I. Miagkov, S. Obraztsov, S. Petrushanko, V. Savrin, A. Snigirev

Skobeltsyn Institute of Nuclear Physics, Lomonosov Moscow State University, Moscow, Russia

V. Blinov [43], Y. Skovpen [43], D. Shtol [43]

Novosibirsk State University (NSU), Novosibirsk, Russia

I. Azhgirey, I. Bayshev, S. Bitioukov, D. Elumakhov, V. Kachanov, A. Kalinin, D. Konstantinov, V. Krychkine, V. Petrov, R. Ryutin, A. Sobol, S. Troshin, N. Tyurin, A. Uzunian, A. Volkov

State Research Center of Russian Federation, Institute for High Energy Physics, Protvino, Russia

P. Adzic [44], P. Cirkovic, D. Devetak, M. Dordevic, J. Milosevic, V. Rekovic

University of Belgrade, Faculty of Physics and Vinca Institute of Nuclear Sciences, Belgrade, Serbia

J. Alcaraz Maestre, M. Barrio Luna, M. Cerrada, N. Colino, B. De La Cruz, A. Delgado Peris, A. Escalante Del Valle, C. Fernandez Bedoya, J.P. Fernández Ramos, J. Flix, M.C. Fouz, P. Garcia-Abia, O. Gonzalez Lopez, S. Goy Lopez, J.M. Hernandez, M.I. Josa, A. Pérez-Calero Yzquierdo, J. Puerta Pelayo, A. Quintario Olmeda, I. Redondo, L. Romero, M.S. Soares, A. Álvarez Fernández

Centro de Investigaciones Energéticas Medioambientales y Tecnológicas (CIEMAT), Madrid, Spain

J.F. de Trocóniz, M. Missiroli, D. Moran

Universidad Autónoma de Madrid, Madrid, Spain

J. Cuevas, C. Erice, J. Fernandez Menendez, I. Gonzalez Caballero, J.R. González Fernández, E. Palencia Cortezon, S. Sanchez Cruz, I. Suárez Andrés, P. Vischia, J.M. Vizan Garcia

Universidad de Oviedo, Oviedo, Spain

I.J. Cabrillo, A. Calderon, B. Chazin Quero, E. Curras, M. Fernandez, J. Garcia-Ferrero, G. Gomez, A. Lopez Virto, J. Marco, C. Martinez Rivero, P. Martinez Ruiz del Arbol, F. Matorras, J. Piedra Gomez, T. Rodrigo, A. Ruiz-Jimeno, L. Scodellaro, N. Trevisani, I. Vila, R. Vilar Cortabitarte

Instituto de Física de Cantabria (IFCA), CSIC-Universidad de Cantabria, Santander, Spain

D. Abbaneo, E. Auffray, P. Baillon, A.H. Ball, D. Barney, M. Bianco, P. Bloch, A. Bocci, C. Botta, T. Camporesi, R. Castello, M. Cepeda, G. Cerminara, E. Chapon, Y. Chen, D. d'Enterria, A. Dabrowski, V. Daponte, A. David, M. De Gruttola, A. De Roeck, E. Di Marco [45], M. Dobson, B. Dorney, T. du Pree, M. Dünser, N. Dupont, A. Elliott-Peisert, P. Everaerts, G. Franzoni, J. Fulcher, W. Funk, D. Gigi, K. Gill, F. Glege, D. Gulhan, S. Gundacker, M. Guthoff, P. Harris, J. Hegeman, V. Innocente, P. Janot, O. Karacheban [19], J. Kieseler, H. Kirschenmann, V. Knünz, A. Kornmayer [16], M.J. Kortelainen, M. Krammer [1], C. Lange, P. Lecoq, C. Lourenço, M.T. Lucchini, L. Malgeri, M. Mannelli, A. Martelli, F. Meijers, J.A. Merlin, S. Mersi, E. Meschi, P. Milenovic [46], F. Moortgat, M. Mulders, H. Neugebauer, S. Orfanelli, L. Orsini, L. Pape, E. Perez, M. Peruzzi, A. Petrilli, G. Petrucciani, A. Pfeiffer, M. Pierini, A. Racz, T. Reis, G. Rolandi [47], M. Rovere, H. Sakulin, C. Schäfer, C. Schwick, M. Seidel, M. Selvaggi, A. Sharma, P. Silva, P. Sphicas [48], J. Steggemann, M. Stoye, M. Tosi, D. Treille, A. Triossi, A. Tsirou, V. Veckalns [49], G.I. Veres [21], M. Verweij, N. Wardle, W.D. Zeuner

CERN, European Organization for Nuclear Research, Geneva, Switzerland

W. Bertl [†], L. Caminada [50], K. Deiters, W. Erdmann, R. Horisberger, Q. Ingram, H.C. Kaestli, D. Kotlinski, U. Langenegger, T. Rohe, S.A. Wiederkehr

Paul Scherrer Institut, Villigen, Switzerland

F. Bachmair, L. Bäni, P. Berger, L. Bianchini, B. Casal, G. Dissertori, M. Dittmar, M. Donegà, C. Grab, C. Heidegger, D. Hits, J. Hoss, G. Kasieczka, T. Klijnsma, W. Lustermann, B. Mangano, M. Marionneau, M.T. Meinhard, D. Meister, F. Micheli, P. Musella, F. Nessi-Tedaldi, F. Pandolfi, J. Pata, F. Pauss, G. Perrin, L. Perrozzi, M. Quittnat, M. Schönenberger, L. Shchutska, V.R. Tavolaro, K. Theofilatos, M.L. Vesterbacka Olsson, R. Wallny, A. Zagozdzinska [36], D.H. Zhu

Institute for Particle Physics, ETH Zurich, Zurich, Switzerland

T.K. Aarrestad, C. Amsler [51], M.F. Canelli, A. De Cosa, S. Donato, C. Galloni, T. Hreus, B. Kilminster, J. Ngadiuba, D. Pinna, G. Rauco, P. Robmann, D. Salerno, C. Seitz, A. Zucchetta

Universität Zürich, Zurich, Switzerland

V. Candelise, T.H. Doan, Sh. Jain, R. Khurana, C.M. Kuo, W. Lin, A. Pozdnyakov, S.S. Yu

National Central University, Chung-Li, Taiwan

Arun Kumar, P. Chang, Y. Chao, K.F. Chen, P.H. Chen, F. Fiori, W.-S. Hou, Y. Hsiung, Y.F. Liu, R.-S. Lu, M. Miñano Moya, E. Paganis, A. Psallidas, J.f. Tsai

National Taiwan University (NTU), Taipei, Taiwan

B. Asavapibhop, K. Kovitanggoon, G. Singh, N. Srimanobhas

Chulalongkorn University, Faculty of Science, Department of Physics, Bangkok, Thailand

A. Adiguzel [52], F. Boran, S. Cerci [53], S. Damarseckin, Z.S. Demiroglu, C. Dozen, I. Dumanoglu,

S. Girgis, G. Gokbulut, Y. Guler, I. Hos [54], E.E. Kangal [55], O. Kara, A. Kayis Topaksu, U. Kiminsu, M. Oglakci, G. Onengut [56], K. Ozdemir [57], D. Sunar Cerci [53], B. Tali [53], S. Turkcapar, I.S. Zorbakir, C. Zorbilmez

Çukurova University, Physics Department, Science and Art Faculty, Adana, Turkey

B. Bilin, G. Karapinar [58], K. Ocalan [59], M. Yalvac, M. Zeyrek

Middle East Technical University, Physics Department, Ankara, Turkey

E. Gülmez, M. Kaya [60], O. Kaya [61], S. Tekten, E.A. Yetkin [62]

Bogazici University, Istanbul, Turkey

M.N. Agaras, S. Atay, A. Cakir, K. Cankocak

Istanbul Technical University, Istanbul, Turkey

B. Grynyov

Institute for Scintillation Materials of National Academy of Science of Ukraine, Kharkov, Ukraine

L. Levchuk, P. Sorokin

National Scientific Center, Kharkov Institute of Physics and Technology, Kharkov, Ukraine

R. Aggleton, F. Ball, L. Beck, J.J. Brooke, D. Burns, E. Clement, D. Cussans, O. Davignon, H. Flacher, J. Goldstein, M. Grimes, G.P. Heath, H.F. Heath, J. Jacob, L. Kreczko, C. Lucas, D.M. Newbold [63], S. Paramesvaran, A. Poll, T. Sakuma, S. Seif El Nasr-storey, D. Smith, V.J. Smith

University of Bristol, Bristol, United Kingdom

K.W. Bell, A. Belyaev [64], C. Brew, R.M. Brown, L. Calligaris, D. Cieri, D.J.A. Cockerill, J.A. Coughlan, K. Harder, S. Harper, E. Olaiya, D. Petyt, C.H. Shepherd-Themistocleous, A. Thea, I.R. Tomalin, T. Williams

Rutherford Appleton Laboratory, Didcot, United Kingdom

R. Bainbridge, S. Breeze, O. Buchmuller, A. Bundock, S. Casasso, M. Citron, D. Colling, L. Corpe, P. Dauncey, G. Davies, A. De Wit, M. Della Negra, R. Di Maria, A. Elwood, Y. Haddad, G. Hall, G. Iles, T. James, R. Lane, C. Laner, L. Lyons, A.-M. Magnan, S. Malik, L. Mastrolorenzo, T. Matsushita, J. Nash, A. Nikitenko [6], V. Palladino, M. Pesaresi, D.M. Raymond, A. Richards, A. Rose, E. Scott, C. Seez, A. Shtipliyski, S. Summers, A. Tapper, K. Uchida, M. Vazquez Acosta [65], T. Virdee [16], D. Winterbottom, J. Wright, S.C. Zenz

Imperial College, London, United Kingdom

J.E. Cole, P.R. Hobson, A. Khan, P. Kyberd, I.D. Reid, P. Symonds, L. Teodorescu, M. Turner

Brunel University, Uxbridge, United Kingdom

A. Borzou, K. Call, J. Dittmann, K. Hatakeyama, H. Liu, N. Pastika, C. Smith

Baylor University, Waco, USA

R. Bartek, A. Dominguez

Catholic University of America, Washington DC, USA

A. Buccilli, S.I. Cooper, C. Henderson, P. Rumerio, C. West

The University of Alabama, Tuscaloosa, USA

D. Arcaro, A. Avetisyan, T. Bose, D. Gastler, D. Rankin, C. Richardson, J. Rohlf, L. Sulak, D. Zou

Boston University, Boston, USA

G. Benelli, D. Cutts, A. Garabedian, J. Hakala, U. Heintz, J.M. Hogan, K.H.M. Kwok, E. Laird, G. Landsberg, Z. Mao, M. Narain, J. Pazzini, S. Piperov, S. Sagir, R. Syarif, D. Yu

Brown University, Providence, USA

R. Band, C. Brainerd, D. Burns, M. Calderon De La Barca Sanchez, M. Chertok, J. Conway, R. Conway, P.T. Cox, R. Erbacher, C. Flores, G. Funk, M. Gardner, W. Ko, R. Lander, C. Mclean, M. Mulhearn, D. Pellett, J. Pilot, S. Shalhout, M. Shi, J. Smith, M. Squires, D. Stolp, K. Tos, M. Tripathi, Z. Wang

University of California, Davis, Davis, USA

M. Bachtis, C. Bravo, R. Cousins, A. Dasgupta, A. Florent, J. Hauser, M. Ignatenko, N. Mccoll, D. Saltzberg, C. Schnaible, V. Valuev

University of California, Los Angeles, USA

E. Bouvier, K. Burt, R. Clare, J. Ellison, J.W. Gary, S.M.A. Ghiasi Shirazi, G. Hanson, J. Heilman, P. Jandir, E. Kennedy, F. Lacroix, O.R. Long, M. Olmedo Negrete, M.I. Paneva, A. Shrinivas, W. Si, L. Wang, H. Wei, S. Wimpenny, B.R. Yates

University of California, Riverside, Riverside, USA

J.G. Branson, S. Cittolin, M. Derdzinski, B. Hashemi, A. Holzner, D. Klein, G. Kole, V. Krutelyov, J. Letts, I. Macneill, M. Masciovecchio, D. Olivito, S. Padhi, M. Pieri, M. Sani, V. Sharma, S. Simon, M. Tadel, A. Vartak, S. Wasserbaech [66], J. Wood, F. Würthwein, A. Yagil, G. Zevi Della Porta

University of California, San Diego, La Jolla, USA

N. Amin, R. Bhandari, J. Bradmiller-Feld, C. Campagnari, A. Dishaw, V. Dutta, M. Franco Sevilla, C. George, F. Golf, L. Gouskos, J. Gran, R. Heller, J. Incandela, S.D. Mullin, A. Ovcharova, H. Qu, J. Richman, D. Stuart, I. Suarez, J. Yoo

University of California, Santa Barbara – Department of Physics, Santa Barbara, USA

D. Anderson, J. Bendavid, A. Bornheim, J.M. Lawhorn, H.B. Newman, T. Nguyen, C. Pena, M. Spiropulu, J.R. Vlimant, S. Xie, Z. Zhang, R.Y. Zhu

California Institute of Technology, Pasadena, USA

M.B. Andrews, T. Ferguson, T. Mudholkar, M. Paulini, J. Russ, M. Sun, H. Vogel, I. Vorobiev, M. Weinberg

Carnegie Mellon University, Pittsburgh, USA

J.P. Cumalat, W.T. Ford, F. Jensen, A. Johnson, M. Krohn, S. Leontsinis, T. Mulholland, K. Stenson, S.R. Wagner

University of Colorado Boulder, Boulder, USA

J. Alexander, J. Chaves, J. Chu, S. Dittmer, K. Mcdermott, N. Mirman, J.R. Patterson, A. Rinkevicius, A. Ryd, L. Skinnari, L. Soffi, S.M. Tan, Z. Tao, J. Thom, J. Tucker, P. Wittich, M. Zientek

Cornell University, Ithaca, USA

S. Abdullin, M. Albrow, G. Apollinari, A. Apresyan, A. Apyan, S. Banerjee, L.A.T. Bauerdick, A. Beretvas, J. Berryhill, P.C. Bhat, G. Bolla, K. Burkett, J.N. Butler, A. Canepa, G.B. Cerati, H.W.K. Cheung, F. Chlebana, M. Cremonesi, J. Duarte, V.D. Elvira, J. Freeman, Z. Gecse, E. Gottschalk, L. Gray, D. Green, S. Grünendahl, O. Gutsche, R.M. Harris, S. Hasegawa, J. Hirschauer, Z. Hu, B. Jayatilaka, S. Jindariani, M. Johnson, U. Joshi, B. Klima, B. Kreis, S. Lammel, D. Lincoln, R. Lipton, M. Liu, T. Liu, R. Lopes De Sá, J. Lykken, K. Maeshima, N. Magini, J.M. Marraffino, S. Maruyama, D. Mason, P. McBride, P. Merkel, S. Mrenna, S. Nahn, V. O'Dell, K. Pedro, O. Prokofyev, G. Rakness, L. Ristori, B. Schneider, E. Sexton-Kennedy, A. Soha, W.J. Spalding, L. Spiegel, S. Stoynev, J. Strait, N. Strobbe, L. Taylor, S. Tkaczyk, N.V. Tran, L. Uplegger, E.W. Vaandering,

C. Vernieri, M. Verzocchi, R. Vidal, M. Wang, H.A. Weber, A. Whitbeck

Fermi National Accelerator Laboratory, Batavia, USA

D. Acosta, P. Avery, P. Bortignon, D. Bourilkov, A. Brinkerhoff, A. Carnes, M. Carver, D. Curry, S. Das, R.D. Field, I.K. Furic, J. Konigsberg, A. Korytov, K. Kotov, P. Ma, K. Matchev, H. Mei, G. Mitselmakher, D. Rank, D. Sperka, N. Terentyev, L. Thomas, J. Wang, S. Wang, J. Yelton

University of Florida, Gainesville, USA

Y.R. Joshi, S. Linn, P. Markowitz, J.L. Rodriguez

Florida International University, Miami, USA

A. Ackert, T. Adams, A. Askew, S. Hagopian, V. Hagopian, K.F. Johnson, T. Kolberg, G. Martinez, T. Perry, H. Prosper, A. Saha, A. Santra, R. Yohay

Florida State University, Tallahassee, USA

M.M. Baarmand, V. Bhopatkar, S. Colafranceschi, M. Hohlmann, D. Noonan, T. Roy, F. Yumiceva

Florida Institute of Technology, Melbourne, USA

M.R. Adams, L. Apanasevich, D. Berry, R.R. Betts, R. Cavanaugh, X. Chen, O. Evdokimov, C.E. Gerber, D.A. Hangal, D.J. Hofman, K. Jung, J. Kamin, I.D. Sandoval Gonzalez, M.B. Tonjes, H. Trauger, N. Varelas, H. Wang, Z. Wu, J. Zhang

University of Illinois at Chicago (UIC), Chicago, USA

B. Bilki [67], W. Clarida, K. Dilsiz [68], S. Durgut, R.P. Gandrajula, M. Haytmyradov, V. Khristenko, J.-P. Merlo, H. Mermerkaya [69], A. Mestvirishvili, A. Moeller, J. Nachtman, H. Ogul [70], Y. Onel, F. Ozok [71], A. Penzo, C. Snyder, E. Tiras, J. Wetzel, K. Yi

The University of Iowa, Iowa City, USA

B. Blumenfeld, A. Cocoros, N. Eminizer, D. Fehling, L. Feng, A.V. Gritsan, P. Maksimovic, J. Roskes, U. Sarica, M. Swartz, M. Xiao, C. You

Johns Hopkins University, Baltimore, USA

A. Al-bataineh, P. Baringer, A. Bean, S. Boren, J. Bowen, J. Castle, S. Khalil, A. Kropivnitskaya, D. Majumder, W. Mcbrayer, M. Murray, C. Royon, S. Sanders, E. Schmitz, R. Stringer, J.D. Tapia Takaki, Q. Wang

The University of Kansas, Lawrence, USA

A. Ivanov, K. Kaadze, Y. Maravin, A. Mohammadi, L.K. Saini, N. Skhirtladze, S. Toda

Kansas State University, Manhattan, USA

F. Rebassoo, D. Wright

Lawrence Livermore National Laboratory, Livermore, USA

C. Anelli, A. Baden, O. Baron, A. Belloni, B. Calvert, S.C. Eno, C. Ferraioli, N.J. Hadley, S. Jabeen, G.Y. Jeng, R.G. Kellogg, J. Kunkle, A.C. Mignerey, F. Ricci-Tam, Y.H. Shin, A. Skuja, S.C. Tonwar

University of Maryland, College Park, USA

D. Abercrombie, B. Allen, V. Azzolini, R. Barbieri, A. Baty, R. Bi, S. Brandt, W. Busza, I.A. Cali, M. D'Alfonso, Z. Demiragli, G. Gomez Ceballos, M. Goncharov, D. Hsu, Y. Iiyama, G.M. Innocenti, M. Klute, D. Kovalskyi, Y.S. Lai, Y.-J. Lee, A. Levin, P.D. Luckey, B. Maier, A.C. Marini, C. Mcginn,

C. Mironov, S. Narayanan, X. Niu, C. Paus, C. Roland, G. Roland, J. Salfeld-Nebgen, G.S.F. Stephans, K. Tatar, D. Velicanu, J. Wang, T.W. Wang, B. Wyslouch

Massachusetts Institute of Technology, Cambridge, USA

A.C. Benvenuti, R.M. Chatterjee, A. Evans, P. Hansen, S. Kalafut, Y. Kubota, Z. Lesko, J. Mans, S. Nourbakhsh, N. Ruckstuhl, R. Rusack, J. Turkewitz

University of Minnesota, Minneapolis, USA

J.G. Acosta, S. Oliveros

University of Mississippi, Oxford, USA

E. Avdeeva, K. Bloom, D.R. Claes, C. Fangmeier, R. Gonzalez Suarez, R. Kamalieddin, I. Kravchenko, J. Monroy, J.E. Siado, G.R. Snow, B. Stieger

University of Nebraska-Lincoln, Lincoln, USA

M. Alyari, J. Dolen, A. Godshalk, C. Harrington, I. Iashvili, D. Nguyen, A. Parker, S. Rappoccio, B. Roozbahani

State University of New York at Buffalo, Buffalo, USA

G. Alverson, E. Barberis, A. Hortiangtham, A. Massironi, D.M. Morse, D. Nash, T. Orimoto, R. Teixeira De Lima, D. Trocino, D. Wood

Northeastern University, Boston, USA

S. Bhattacharya, O. Charaf, K.A. Hahn, N. Mucia, N. Odell, B. Pollack, M.H. Schmitt, K. Sung, M. Trovato, M. Velasco

Northwestern University, Evanston, USA

N. Dev, M. Hildreth, K. Hurtado Anampa, C. Jessop, D.J. Karmgard, N. Kellams, K. Lannon, N. Loukas, N. Marinelli, F. Meng, C. Mueller, Y. Musienko [37], M. Planer, A. Reinsvold, R. Ruchti, G. Smith, S. Taroni, M. Wayne, M. Wolf, A. Woodard

University of Notre Dame, Notre Dame, USA

J. Alimena, L. Antonelli, B. Bylsma, L.S. Durkin, S. Flowers, B. Francis, A. Hart, C. Hill, W. Ji, B. Liu, W. Luo, D. Puigh, B.L. Winer, H.W. Wulsin

The Ohio State University, Columbus, USA

A. Benaglia, S. Cooperstein, O. Driga, P. Elmer, J. Hardenbrook, P. Hebda, S. Higginbotham, D. Lange, J. Luo, D. Marlow, K. Mei, I. Ojalvo, J. Olsen, C. Palmer, P. Piroué, D. Stickland, C. Tully

Princeton University, Princeton, USA

S. Malik, S. Norberg

University of Puerto Rico, Mayaguez, USA

A. Barker, V.E. Barnes, S. Folgueras, L. Gutay, M.K. Jha, M. Jones, A.W. Jung, A. Khatiwada, D.H. Miller, N. Neumeister, C.C. Peng, J.F. Schulte, J. Sun, F. Wang, W. Xie

Purdue University, West Lafayette, USA

T. Cheng, N. Parashar, J. Stupak

Purdue University Northwest, Hammond, USA

A. Adair, B. Akgun, Z. Chen, K.M. Ecklund, F.J.M. Geurts, M. Guilbaud, W. Li, B. Michlin, M. Northup, B.P. Padley, J. Roberts, J. Rorie, Z. Tu, J. Zabel

Rice University, Houston, USA

A. Bodek, P. de Barbaro, R. Demina, Y.t. Duh, T. Ferbel, M. Galanti, A. Garcia-Bellido, J. Han, O. Hindrichs, A. Khukhunaishvili, K.H. Lo, P. Tan, M. Verzetti

University of Rochester, Rochester, USA

R. Ciesielski, K. Goulianos, C. Mesropian

The Rockefeller University, New York, USA

A. Agapitos, J.P. Chou, Y. Gershtein, T.A. Gómez Espinosa, E. Halkiadakis, M. Heindl, E. Hughes, S. Kaplan, R. Kunnawalkam Elayavalli, S. Kyriacou, A. Lath, R. Montalvo, K. Nash, M. Osherson, H. Saka, S. Salur, S. Schnetzer, D. Sheffield, S. Somalwar, R. Stone, S. Thomas, P. Thomassen, M. Walker

Rutgers, The State University of New Jersey, Piscataway, USA

A.G. Delannoy, M. Foerster, J. Heideman, G. Riley, K. Rose, S. Spanier, K. Thapa

University of Tennessee, Knoxville, USA

O. Bouhali [72], A. Castaneda Hernandez [72], A. Celik, M. Dalchenko, M. De Mattia, A. Delgado, S. Dildick, R. Eusebi, J. Gilmore, T. Huang, T. Kamon [73], R. Mueller, Y. Pakhotin, R. Patel, A. Perloff, L. Perniè, D. Rathjens, A. Safonov, A. Tatarinov, K.A. Ulmer

Texas A&M University, College Station, USA

N. Akchurin, J. Damgov, F. De Guio, P.R. Dudero, J. Faulkner, E. Gurpinar, S. Kunori, K. Lamichhane, S.W. Lee, T. Libeiro, T. Peltola, S. Undleeb, I. Volobouev, Z. Wang

Texas Tech University, Lubbock, USA

S. Greene, A. Gurrola, R. Janjam, W. Johns, C. Maguire, A. Melo, H. Ni, P. Sheldon, S. Tuo, J. Velkovska, Q. Xu

Vanderbilt University, Nashville, USA

M.W. Arenton, P. Barria, B. Cox, R. Hirosky, A. Ledovskoy, H. Li, C. Neu, T. Sinthuprasith, X. Sun, Y. Wang, E. Wolfe, F. Xia

University of Virginia, Charlottesville, USA

R. Harr, P.E. Karchin, J. Sturdy, S. Zaleski

Wayne State University, Detroit, USA

M. Brodski, J. Buchanan, C. Caillol, S. Dasu, L. Dodd, S. Duric, B. Gomber, M. Grothe, M. Herndon, A. Hervé, U. Hussain, P. Klabbers, A. Lanaro, A. Levine, K. Long, R. Loveless, G.A. Pierro, G. Polese, T. Ruggles, A. Savin, N. Smith, W.H. Smith, D. Taylor, N. Woods

University of Wisconsin – Madison, Madison, WI, USA

[10] Now at Fayoum University, El-Fayoum, Egypt.
[11] Also at British University in Egypt, Cairo, Egypt.
[12] Now at Ain Shams University, Cairo, Egypt.
[13] Also at Université de Haute Alsace, Mulhouse, France.
[14] Also at Skobeltsyn Institute of Nuclear Physics, Lomonosov Moscow State University, Moscow, Russia.
[15] Also at Tbilisi State University, Tbilisi, Georgia.
[16] Also at CERN, European Organization for Nuclear Research, Geneva, Switzerland.
[17] Also at RWTH Aachen University, III. Physikalisches Institut A, Aachen, Germany.
[18] Also at University of Hamburg, Hamburg, Germany.
[19] Also at Brandenburg University of Technology, Cottbus, Germany.
[20] Also at Institute of Nuclear Research ATOMKI, Debrecen, Hungary.
[21] Also at MTA-ELTE Lendület CMS Particle and Nuclear Physics Group, Eötvös Loránd University, Budapest, Hungary.
[22] Also at Institute of Physics, University of Debrecen, Debrecen, Hungary.
[23] Also at Indian Institute of Technology Bhubaneswar, Bhubaneswar, India.
[24] Also at Institute of Physics, Bhubaneswar, India.
[25] Also at University of Visva-Bharati, Santiniketan, India.
[26] Also at University of Ruhuna, Matara, Sri Lanka.
[27] Also at Isfahan University of Technology, Isfahan, Iran.
[28] Also at Yazd University, Yazd, Iran.
[29] Also at Plasma Physics Research Center, Science and Research Branch, Islamic Azad University, Tehran, Iran.
[30] Also at Università degli Studi di Siena, Siena, Italy.
[31] Also at INFN Sezione di Milano-Bicocca; Università di Milano-Bicocca, Milano, Italy.
[32] Also at Purdue University, West Lafayette, USA.
[33] Also at International Islamic University of Malaysia, Kuala Lumpur, Malaysia.
[34] Also at Malaysian Nuclear Agency, MOSTI, Kajang, Malaysia.
[35] Also at Consejo Nacional de Ciencia y Tecnología, Mexico city, Mexico.
[36] Also at Warsaw University of Technology, Institute of Electronic Systems, Warsaw, Poland.
[37] Also at Institute for Nuclear Research, Moscow, Russia.
[38] Now at National Research Nuclear University 'Moscow Engineering Physics Institute' (MEPhI), Moscow, Russia.
[39] Also at St. Petersburg State Polytechnical University, St. Petersburg, Russia.
[40] Also at University of Florida, Gainesville, USA.
[41] Also at P.N. Lebedev Physical Institute, Moscow, Russia.
[42] Also at California Institute of Technology, Pasadena, USA.
[43] Also at Budker Institute of Nuclear Physics, Novosibirsk, Russia.
[44] Also at Faculty of Physics, University of Belgrade, Belgrade, Serbia.
[45] Also at INFN Sezione di Roma; Sapienza Università di Roma, Rome, Italy.
[46] Also at University of Belgrade, Faculty of Physics and Vinca Institute of Nuclear Sciences, Belgrade, Serbia.
[47] Also at Scuola Normale e Sezione dell'INFN, Pisa, Italy.
[48] Also at National and Kapodistrian University of Athens, Athens, Greece.
[49] Also at Riga Technical University, Riga, Latvia.
[50] Also at Universität Zürich, Zurich, Switzerland.
[51] Also at Stefan Meyer Institute for Subatomic Physics (SMI), Vienna, Austria.
[52] Also at Istanbul University, Faculty of Science, Istanbul, Turkey.
[53] Also at Adiyaman University, Adiyaman, Turkey.
[54] Also at Istanbul Aydin University, Istanbul, Turkey.
[55] Also at Mersin University, Mersin, Turkey.
[56] Also at Cag University, Mersin, Turkey.
[57] Also at Piri Reis University, Istanbul, Turkey.
[58] Also at Izmir Institute of Technology, Izmir, Turkey.
[59] Also at Necmettin Erbakan University, Konya, Turkey.
[60] Also at Marmara University, Istanbul, Turkey.
[61] Also at Kafkas University, Kars, Turkey.
[62] Also at Istanbul Bilgi University, Istanbul, Turkey.
[63] Also at Rutherford Appleton Laboratory, Didcot, United Kingdom.
[64] Also at School of Physics and Astronomy, University of Southampton, Southampton, United Kingdom.
[65] Also at Instituto de Astrofísica de Canarias, La Laguna, Spain.
[66] Also at Utah Valley University, Orem, USA.
[67] Also at Beykent University, Istanbul, Turkey.
[68] Also at Bingol University, Bingol, Turkey.
[69] Also at Erzincan University, Erzincan, Turkey.
[70] Also at Sinop University, Sinop, Turkey.
[71] Also at Mimar Sinan University, Istanbul, Istanbul, Turkey.
[72] Also at Texas A&M University at Qatar, Doha, Qatar.
[73] Also at Kyungpook National University, Daegu, Republic of Korea.